

Final degree project

**Degree in Industrial Technology engineering**

**Recovery of Rare Earth elements  
through chelating resin**

**MEMÒRIA**

**Autor:** Wenbo Ruan  
**Director:** Jose Luis Cortina  
**Ponent:**  
**Convocatòria:** 7 2016



Escola Tècnica Superior  
d'Enginyeria Industrial de Barcelona



## Summary

Abstract .....	4
1. Introduction .....	5
1.1. Industrial uses of RE .....	5
1.2. REE Sources .....	7
1.2.1. Primary sources .....	7
1.2.2. Secondary sources .....	9
1.3. RRE Extraction technologies .....	12
Gravity separation .....	12
Magnetic separation .....	12
Electrostatic separation .....	13
Froth flotation .....	13
Photochemical separation .....	13
Solvent extraction .....	13
Ion exchange .....	17
Supercritical extraction .....	19
2. Experimental methodologies .....	19
2.1. Materials .....	19
2.2. REE containing samples: acidic mine waters and calcium rich mine wastes .....	20
Analysis methodologies .....	23
2.3. Metals extraction methodologies .....	24
Determination of the equilibration time .....	24
Effect of $-\log [H^+]$ on REE and transition metal extraction .....	24
Effect of mass of resin on REE and transition metals extraction .....	24
Separation of REE from transition metals .....	24
Resin Saturation assays .....	24
3. Results and discussion .....	25
3.1. Characterization of secondary resources samples .....	25
3.2. Metal extraction kinetic with ion-exchange resins S957 and TP207 .....	29
3.3. Extraction dependence of REE on solution acidity .....	31
3.4. Evaluation of resin concentration on metal extraction reactions. ....	35
3.5. Evaluation of the Separation factors of REE from transition metal .....	38
3.6. Identification of metal extraction reactions for TP207 and S957 resins .....	44
3.7. Resin saturation assays using extraction cycles .....	50

Project planning and economical evaluation .....	55
Environmental assessment/sustainability issues .....	57
Conclusions .....	58
Acknowledgments .....	58
Reference .....	59
Annex .....	63

## Abstract

The market of rare earths (RE); crucial elements needed in every field of industry; is currently being controlled by China since middle of the past century. China controls about 95% of global rare earths production and holds half the world reserves of RE. For years, China controlled the exportation of RE and in 2010 abruptly reduced its exportation quota creating supply disruptions. For this reason, rare-earth elements (REE) have been considered by the EU as critical elements and it is a need to extract them from secondary sources.

As secondary resources include urban wastes (e.g. fluorescent lamps, batteries, TV tubes and flat screens, etc.) and industrial (e.g. magnets) and mining wastes (e.g. mining tailings, clays, etc.). The concentration of RE in most of the secondary sources is below 1% and then recovery from such types of wastes include the combination of hydrometallurgical and pyrometallurgical processing technologies. For hydrometallurgical processing, after proper dissolution of the raw wastes with appropriate leaching solutions REE elements should be separated from transition metals (TM). REE streams then are concentrated by solvent extraction or ion-exchange as previous step to subsequent steps of separation and purification.

In this study effluents collected in abandoned mines of the Odiel basin (Huelva) suffering acid-mine drainage and solid wastes generated in the on-site treatment of such effluents have been evaluated as potential secondary REE resources. Liquid samples and solid wastes have been characterized chemically and the composition on REE and transition metals has been determined. In a second stage two ion exchange resins, one containing an aminophosphonic and sulphonic acid functional groups (Purolite S957) and one containing an imino-diacetic group (TP207) have been evaluated as potential materials for recovery of REE from moderate to strongly acidic solutions (from 0.01 to 10 M  $\text{H}_2\text{SO}_4$ ). The capacity and the selectivity separation factors with TR metals as a function of resin dose and solution acidity have been determined using batch experiments. As a general trend REE elements are better extracted at more strong acidities than TM and when compared both resins TP207 shown higher extraction capacity than S957. Both for resins metal extraction processes are faster for S957 where after 15-30 minutes the system reached equilibrium. Contrary, the metal extraction reactions for TP207 are slower and more that 2-3 hours were needed to reach equilibrium. The, higher kinetics of S957 resins should be associated to the presence of sulfonic groups.

The REE extraction had been proven to be possible with both of the resin, with upstanding result such as 100% REE extraction for resin S957 and up to 60% of REE extraction for resin TP 207. However, also TM were extracted even a very acidic solutions, and the differences found with REE are not enough to achieve the needed separation factors. The high levels of Fe and Cu in the studied samples seems to be one of the main limitations to achieve the required selectivity.

## 1. Introduction

Rare earths (RE), a term used to design the lanthanides in row 3 of the periodic table, elements included in this group are: Scandium (Sc), Yttrium (Y), Lanthanum (La), Cerium (Ce), Praseodymium (Pr), Neodymium (Nd), Promethium (Pm), Samarium (Sm), Europium (Eu), Gadolinium (Gd), Terbium (Tb), Dysprosium (Dy), Holmium (Ho), Erbium (Er), Thulium (Tm), Ytterbium (Yb) and Lutetium (Lu).

However the name “rare earths” may be misleading giving the fact those elements are relatively abundant on Earth’s crust, nevertheless hardly happen in minerals at high contents and are mostly dispersed ([F. Xie et al, 2014](#)).

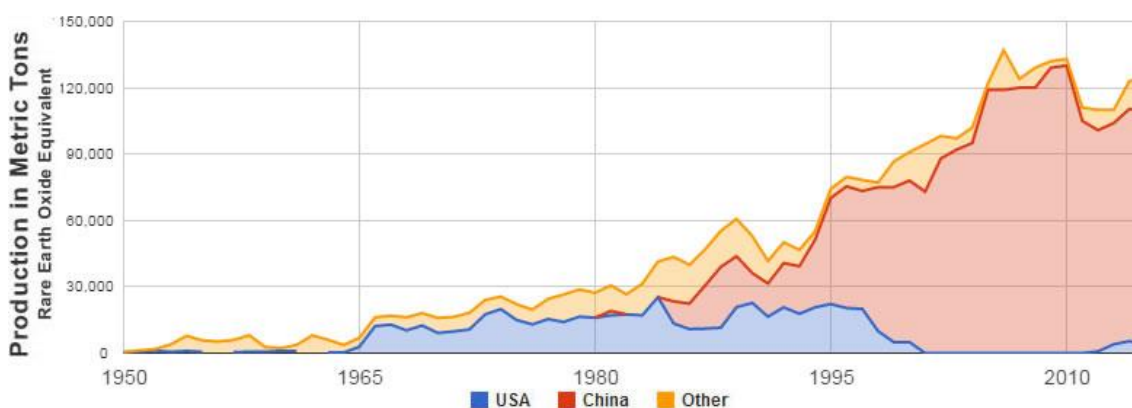


Figure 1 Production of REE in the world through time years. (reference should be provided)

During the recent years, the demand of rare earths (REs) have been increasing drastically, just like its production, however its demand had not been always like prior to 1965. At this point occurred the first explosion with the color television entering to the market, since this mentioned product required Europium, and with that the Mountain Pass in California, became the world largest producer ([Tse, 2011](#)). With China entering the rare earths market with such a cheap prize, that the mountain Pass was unable to compete and was doomed to its end ([REE - Rare Earth Elements and their Uses, <http://geology.com/articles/rare-earth-elements/>](#) ).

### 1.1. Industrial uses of RE

RE metals and their compounds are in high demand for chemical, electrical, magnetic and optical properties ([Xie, 2014](#)). They commonly used in metallurgical, petroleum, textiles and agriculture sector in ([Commercial Applications for Rare Earth Technology, <http://reitausa.org>](#)) in early years, and recently they also have become decisive and essential to cutting-edge technology, such as hybrid car, wind turbines, compact fluorescent lights, flats screen, mobile phones, disc drives and medical and military technology ([Goonan. 2011](#)). One good example of the use of rare earth as catalysts in petroleum refining, ([Goonan. 2011](#)) is the application in the cracking process. As this process depends on the control of temperature, pressure and the presence of a suitable catalysis to provide active reaction sites on which the desired reactions can take place.

Another outstanding use is in magnets. Magnets are alloys of rare earth and transition metals like iron, nickel and cobalt ([Masari et al., 2013](#)). The most used nowadays are the neodymium

magnet, with some exception for the higher Curie point of Samarium-cobalt magnet ([Brown et al., 2002](#)).

REEs have its own field of application, and a list of applications is provided in Table 1 and a detailed list for Dysprosium is described in table 2 ([Constantinides et al. 2011](#)).

*Table 1 Examples of industrial uses of REE.*

REE application	La	Ce	Pr	Nd	Sm	Eu	Gd	Tb	Dy	Y	Other
Magnet	-	-	23,4	69,4	-	-	2,0	0,2	5,0	-	-
Battery alloys	50,0	33,4	3,3	10,0	3,3	-	-	-	-	-	-
Metals alloys	26,0	52,0	5,5	16,5	-	-	-	-	-	-	-
Auto catalysis	5,0	90,0	2,0	3,0	-	-	-	-	-	-	-
Petroleum refining	90,0	10,0	-	-	-	-	-	-	-	-	-
Polishing	31,5	65,0	3,5	-	-	-	-	-	-	-	-
Glass additives	24,0	66,0	1,0	3,0	-	-	-	-	-	2,0	4,0
phosphors	8,5	11,0	-	-	-	4,9	1,8	4,6	-	69,2	-
Ceramics	17,0	12,0	6,0	13,0	-	-	-	-	-	53,0	-
Other	19,0	39,0	4,0	15,0	2,0	-	1,0	-	-	19,0	-

*Table 2 Content in Dy of some of the most common electronics ([Constantinide et a., 2011](#))*

Application	Typical Dy content (%) <sup>a</sup>
Hybrid and electric cars	8,7
Generators	6,4
Wave guides: TWT, ondulators, wigglers	4,1
Electric bikes and storage systems	4,1
Magnetic brakes, magnetically levitated transport	4,1
Motors, industrial, cars, wind turbines.	4,1
Pipe inspection Systems, relays and switchhes	4,1
Reprographics, torque and coupled drives	4,1
Gauges, hysteresis clutch, magnetic separators	2,8
Magnetic refrigerators, MRI scanners, sensors	1,4

<sup>a</sup> % of Dy compared to the other rare earths.

## 1.2. REE Sources

As mentioned previously, RE are relatively abundant on the Earth, but only in small concentration. There are, however, some minerals with high concentrations of REE and mines of those minerals, are in fact the main source of RE. Giving the fact the mines of the mentioned mineral are scale different sources of lower RE concentration are also taking into account.

### 1.2.1. Primary sources

#### *Bastanasite.*

Bastanasite is a fluorocarbonate mineral with a REE content of approximately 70% rare earth oxide (REO), which the main elements are Ce, La, Pr and Nd (aprox 97.95%). In the last 50 years bastanasite has been replacing monazite all along, and the reason is due to the discovery and development of the world largest RE mine, the Bayan Obo mine in China and the Mountain Pass mine in the US ([Jordens et al, \(2013\)](#)). The separation process used on this mineral in order to obtain REE consist in employing numerous operations, including gravity and magnetic concentration. Notable occurrence include the carbonatite-hosted bastnesite deposit at Mountain Pass, California, several bastnesite deposits in Sichuan (China) and the massive deposit in Bayan Obo (China) ([Xie et al, 2014](#)). A summary of carbonate and halide minerals is provided in Tables 3 and 4.

*Table 3 Carbonate REE bearing minerals. Adapted from (Anthony et al., 2001; Long et al., 2010; Rosenblum and Brownfield, 1999)*

Mineral name	Chemical formula	Density(g/cm3)	Magnetic properties	Weight percent		
				REO	ThO2	UO2
Carbonates			Para/diamagnetic			
Ancylite (Ce)	Sr(Ce,La)(CO3)2OH_H2O	3,82-4,30	n/a	46-53	0-0,4	0,1
Ancylite (La)	Sr(La,Ce)(CO3)2OH_H2O	3,69	n/a	46-53	0-0,4	0,1
Bastnäsite (Ce)	(Ce,La)(CO3)F	4,90-5,20	Paramagnetic	70-74	0-0,3	0,09
Bastnäsite (La)	(La,Ce)(CO3)F	n/a	Paramagnetic	70-74	0-0,3	0,09
Bastnäsite (Y)	Y(CO3)F	3,90-4,00	Paramagnetic	70-74	0-0,3	0,09
Calcio-ancylite (Ce)	(Ca,Sr)Ce3(CO3)4(OH)3_H2O	3,95	n/a	60	-	-
Calcio-ancylite (Nd)	Ca(Nd,Ce,Gd,Y)3(CO3)4(OH)3_H2O	4,02	n/a	60	-	-
Parisite (Ce)	Ca(Ce,La)2(CO3)3F2	4,33	Paramagnetic	59	0-0,5	0-0,3
Synchysite (Ce)	Ca(Ce,La)(CO3)2F	3,90	n/a	49-52	1,6	-

*Table 4 Halide REE bearing minerals. Adapted from (Anthony et al., 2001; Long et al., 2010; Rosenblum and Brownfield, 1999)*

Mineral name	Chemical formula	Density(g/cm3)	Magnetic properties	Weight percent		
				REO	ThO2	UO2
Halides			Para/diamagnetic			
Fluocerite (Ce)	(Ce,La)F3	5,93	Paramagnetic	-	-	-
Fluocerite (La)	(La,Ce)F3	5,93	Paramagnetic	-	-	-
Fluorite	(Ca,REE)F2	3,18-3,56	Paramagnetic	-	-	-
Gagarinite (Y)	NaCaY(F,Cl)6	4,11-4,29	n/a	-	-	-
Pyrochlore	(Ca,Na,REE)2Nb2O6(OH,F)	4,45-4,90	Paramagnetic	-	-	-
Yttrofluorite	(Ca,Y)F2	n/a	n/a	-	-	-

## Monazite

Monazite is a phosphate mineral, with high resemblance to bastanaseite; monazite has a REO content of over 70%, primarily Ce, La, Pr and Nd. However, monazite also contain small amount of Th and Uranium ([Jordens et al \(2013\)](#)). This mineral can be found in placer deposit, beach sands and other minerals. The main deposit for monazite is beach sands, which are treated with high-capacity gravity separation. The primary mine of monazite are placed in Australia, Brazil, China, India, Malaysia, South Africa, Sri Lanka, Thailand, and the United States ([Xie et alt, 2014](#)). A similar mineral is Xenotime, a Y phosphate mineral with REO content of over 67%, can be found alongside with monazite in lower concentration. A summary of phosphate and oxide based minerals is provided in Tables 5 and 6.

**Table 5** Oxide REE bearing minerals. Adapted from ([Anthony et al., 2001](#); [Long et al., 2010](#); [Rosenblum and Brownfield, 1999](#))

Mineral name	Chemical formula	Density(g/cm3)	Magnetic properties	Weight percent		
				REO	ThO2	UO2
Oxides			Para/diamagnetic			
Anatase	(Ti,REE)O2	3.79–3.97	Diamagnetic	-	-	-
Brannerite	(U,Ca,Y,Ce)(Ti,Fe)2O6	4.20–5.43	Paramagnetic	-	-	-
Cerianite (Ce)	(Ce4+,Th)O2	7.20 (syn)	n/a	-	-	-
Euxenite (Y)	(Y,Ca,Ce,U,Th)(Nb,Ta,Ti)2O6	5.30–5.90	Paramagnetic	-	-	-
Fergusonite (Ce)	(Y,Ca,Ce,U,Th)(Nb,Ta,Ti)2O6	5.45–5.48	Paramagnetic	-	-	-
Fergusonite (Nd)	(Nd,Ce)(Nb,Ti)O4	n/a	Paramagnetic	-	-	-
Fergusonite (Y)	YNbO4	5.60–5.80	Paramagnetic	-	-	-
Loparite (Ce)	(Ce,Na,Ca)(Ti,Nb)O3	4.60–4.89	n/a	-	-	-
Perovskite	(Ca, REE)TiO3	3.98–4.26	Diamagnetic	<37	0-2	0-0,05
Samarskite	(REE,Fe2+,Fe3+,U,Th,Ca)(Nb,Ta,Ti)O4	5.00–5.69	Paramagnetic	-	-	-
Uraninite	(U,Th,Ce)O2	10.63–10.95	Paramagnetic	-	-	-

**Table 6** Silicate REE bearing Minerals. Adapted from ([Anthony et al., 2001](#); [Long et al., 2010](#); [Rosenblum and Brownfield, 1999](#)).

Mineral name	Chemical formula	Density(g/cm3)	Magnetic properties	Weight percent		
				REO	ThO2	UO2
Phosphates			Para/diamagnetic			
Britholite (Ce)	(Ce,Ca)5(SiO4,PO4)3(OH,F)	4.20–4.69	Paramagnetic	56	1,5	-
Britholite (Y)	(Y,Ca)5(SiO4,PO4)3(OH,F)	4.35	Paramagnetic	56	1,5	-
Florencite (Ce)	CeAl3(PO4)2(OH)6	3.45–3.54	n/a	-	1,4	-
Florencite (La)	(La,Ce)Al3(PO4)2(OH)6	3.52	n/a	-	1,4	-
Florencite (La)	(Nd,Ce)Al3(PO4)2(OH)6	3.70 (calc)	n/a	-	1,4	-
Fluorapatite	(Ca,Ce)5(PO4)3F	3.10–3.25	n/a	-	-	-
Gorceixite	(Ba,REE)Al3[(PO4)2(OH)5]_H2O	3.04–3.19	Diamagnetic	-	-	-
Goyazite	SrAl3(PO4)2(OH)5_H2O	3.26	Diamagnetic	-	-	-
Monazite (Ce)	(Ce,La,Nd,Th)PO4	4.98–5.43	Paramagnetic	35-71	0-20	0-16
Monazite (La)	(La,Ce,Nd,Th)PO4	5.17–5.27	Paramagnetic	35-71	0-20	0-16
Monazite (Nd)	(Nd,Ce,La,Th)PO4	5.43 (calc)	Paramagnetic	35-71	0-20	0-16
Xenotime (Y)	YPO4	4.40–5.10	Paramagnetic	52-67	-	0-5



### ***Ion-adsorbed clays***

A very important source of REO, with over 60% of its content in REO coming from Y and little requirement for physical beneficiation needed, can be considered one of the most important source of RE, and can be processed almost directly using hydrometallurgical methods. Some of the most important deposit can be found in Ganzhou, Jiangxi in China ([Yang et al 2013](#)). A summary of silicate based minerals is provided in Tables 7 and 8.

*Table 7 Silicate REE bearing Minerals. Adapted from (Anthony et al., 2001; Long et al., 2010; Rosenblum and Brownfield, 1999).*

Mineral name	Chemical formula	Density(g/cm3)	Magnetic properties	Weight percent		
				REO	ThO2	UO2
Silicate			Para/diamagnetic			
Allanite (Ce)	(Ce,Ca,Y)2(Al,Fe2+,Fe3+)3(SiO4)3(OH)	3.50–4.20	Paramagnetic	3-51	0-3	-
Allanite (Y)	(Y,Ce,Ca)2(Al,Fe3+)3(SiO4)3(OH)	n/a	Paramagnetic	3-51	0-3	-
Cerite (Ce)	Ce9Fe3+[SiO2]6[(SiO3)(OH)](OH)3	4.75	Paramagnetic	-	-	-
Cheralite (Ce)	(Ca,Ce,Th)(P,Si)O4	5.28	n/a	-	<30	-
Eudialyte	Na4(Ca,Ce)2(Fe2+,Mn2+,Y)ZrSi8O22(OH,Cl)2	2.74–3.10	n/a	1-10	-	-
Gadolinite (Ce)	(Ce,La,Nd,Y)2Fe2+Be2Si2O10	4.20	Paramagnetic	-	-	-
Gadolinite (Y)	(Ce,La,Nd,Y)2Fe2+Be2Si2O10	4.36–4.77	Paramagnetic	-	-	-
Steenstrupine (Ce)	Na14Ce6Mn2Fe2(Zr,Th)(Si6O18)2(PO4)7_3H2O	3.38–3.47	n/a	<3	-	-
Thorite	(Th,U)SiO4	6.63–7.20	Paramagnetic	-	-	10-16
Zircon	(Zr,REE)SiO4	4.60–470	Diamagnetic	-	0,1-0,8	-

*Table 8 Content of REE in mines over world in (F. Xie et al (2014) 10–28)*

Element	Bastnäsite		Monazite	Xenotime	High Y REE clay	LOW Y REE clay
	Mountain Pass, USA	Bayan Obo, China				
La (%)	33,8	23,0	17,5	1,2	1,8	43,4
Ce (%)	49,6	50,0	43,7	3,1	0,4	2,4
Pr (%)	4,1	6,2	5,0	0,5	0,7	7,1
Nd (%)	11,2	18,5	17,5	1,6	3,0	30,2
Sm (%)	0,9	0,8	4,9	1,1	2,8	3,9
Eu (%)	0,1	0,2	0,2	Trace	0,1	0,5
Gd (%)	0,2	0,7	6,0	3,5	6,9	4,2
Tb (%)	-	0,1	0,3	0,9	1,3	Trace
Dy (%)	-	0,1	0,9	8,3	7,5	Trace
Ho (%)	-	Trace	0,1	2,0	1,6	Trace
Er (%)	-	Trace	Trace	6,4	4,9	Trace
Tm (%)	-	Trace	Trace	1,1	0,7	Trace
Yb (%)	-	Trace	0,1	6,8	2,5	0,3
Lu (%)	Trace	Trace	Trace	1,0	0,4	0,1
Y (%)	0,1	Trace	2,5	61,0	65	8,0

### **1.2.2. Secondary sources**

Aside from mine containing direct RE mineral, there are other sources from where is possible to obtain those appreciated elements, sources such as wastes and side streams in the mining industries, waste electrical and electronic equipment ([Virolainen 2013](#)), deep sea nodule leach Liquor ([Woo-Nam et alt, 2013](#)), permanent magnet ([Binnemans et al. \(2013\)](#)) among others can serve as example of secondary sources.

### Electronic and electric waste

There are multiple waste that can be used as potential resources for REE; photovoltaic cells, vehicles, catalyst from the petrochemical industry and a long list of scraps, one example would be fluorescent lamp, the fluorescent lamps contain a significant amount of REO in their luminescent or fluorescent powders, in specific Eu, Tb and Y ([Virolainen 2013](#)), being Y the one with the highest concentration while the Eu and Tb have higher price.

### Permanent REE magnet

The most common rare earth magnet are based upon neodymium-iron-boron alloys, as such there are high concentration of Nd in it, as well as small mixture of other REE like Pr, Gd, Tb and Dy ([Binnemans et al. \(2013\)](#)), and there are countless application that requires the usage of this magnet, application such as generators, Magnetic resonance imaging (MRI) scanners, sensors among others. A scheme of the recovery of REE is provided in Figure 2

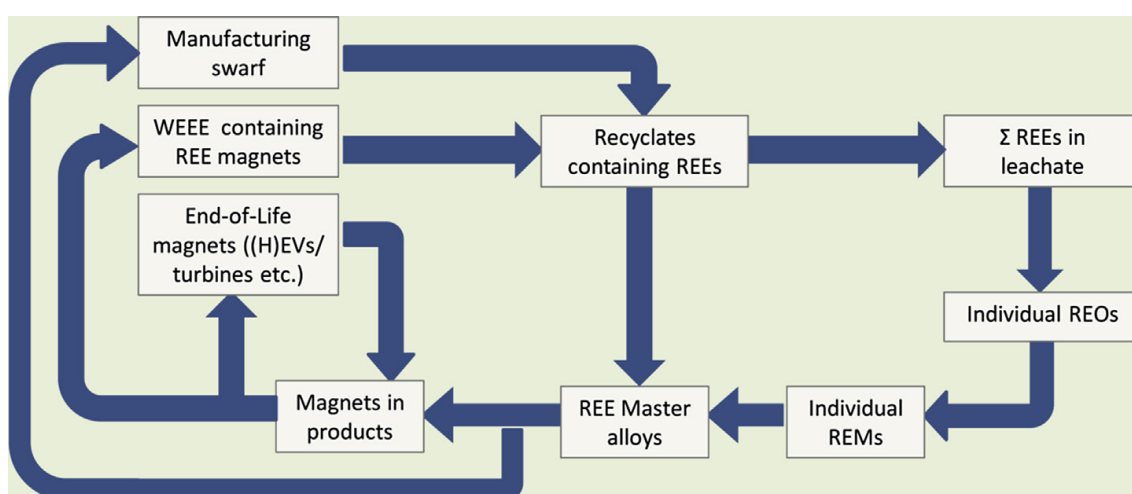


Figure 2 simplified recycling flow sheet for REE magnets, from ([Binnemans et al. \(2013\)](#))

### Deep sea nodule leach liquor

Just like bastnaesite and monazite, deep sea nodules are also minerals bearing REE, unlike the previously mentioned two, are found under water, and they also contain a significant amount of REE which can be recovered using hydrometallurgical methods ([Woo-Nam et al; 2013](#)).

### Mine drainage

It not unusual to find rare earth in mines drainage ([Ayora et al.; 2013](#)), the concentration and element type in it can vary depending on the geological situation where the mine is located. The reasons for the REE enrichment in AMD with respect to the rest of natural waters are grounded in their aqueous geochemistry. A minor part of REE in rocks is concentrated in accessory minerals, such as zircon, monazite or allanite ([Chakhmouradian and Wall, 2012](#)). These minerals do not undergo weathering, and therefore they concentrate in detrital rocks and placers. However, the majority of REE in igneous and sedimentary rocks are occasionally located as major components of carbonates (bastnaesite) and phosphates (monazite), and more commonly as traces in rock forming silicates, such as plagioclase. Weathering of these minerals in conventional soils occurs due to the aggressive action of CO<sub>2</sub> and humic acids. Once in solution, REE in soil pore water remain as trivalent cations or, at neutral to alkaline pH complexed with CO<sub>3</sub><sup>2-</sup> and OH<sup>-</sup>. Due to its large positive charge and ionic potential, trivalent cations are strongly

sorbed onto the negative charged surface of clays, kaolinite and illite, or replace Na and Ca in the interlayer positions of smectites ([Bradbury and Baeyens, 2002; 2009; Coppin et al., 2002; Tertre et al., 2005](#)). As a consequence, REE are mainly concentrated in clays, which become a major reservoir of REE in sedimentary rocks. If the primary rock is rich in REE, weathering clays may become an economical target for mining, such as the residual deposits in South China ([Kynicky et al., 2012](#)). However the main problem consists in the low concentration of the REE which would require a pre-concentration before the beneficiation.

When AMD effluents mix with neutral waters of receiving water bodies (see Figure 3) and the pH increases accordingly, the concentrations of REE are greatly depleted in these mixing zones.



*Figure 3 Schwertmannite (red) and basaluminite (white) precipitates at the mixing zone of Odiel river (left) and the Agrio tributary (right) (ref from C. Ayora, 2016)*

In cases, mixing of AMD-impacted Rivers, such as Tinto and Odiel, with seawater in the estuary also decreases their concentration. Aluminum, Fe and REE transported by the acidic rivers are extensively removed in the estuary where the acidic water is neutralized. The REE removal is due to several simultaneous mechanisms: co-precipitation with oxyhydroxides (mainly Al and Fe), complexation with flocculating humic substances, and sorption to suspended particles ([Astrom et al., 2012](#)). Despite of the mixing, and the lower REE concentrations, the typical MREE enriched pattern of AMD is still recognizable in the estuarine sediments of the Guadiana River, suggesting the forensic possibilities of the REE patterns in AMD impacted sediments (Delgado et al., 2012).

Recently, a critical review on secondary wastes has been provided by ([Binnemans et al., 2013](#)), a summary of different component containing rare earth that can be recycled is provided in table 9.

Table 9 Waste from industry containing REE (Binnemans et al. (2013))

Product life period	Materials stream and application	REEs
Preconsumer production scrap and residues	Magnet swarf and rejected magnets	Nd, Dy, Tb, Pr
	residues arising during metal production/recycling	All
	Postsmelter and electric arc furnace residues	Ce, La, critical REEs
	Industrial residues	All
End-of-life products	Fluorescent lamps	Eu, Tb, Y
	Compact fluorescent lamps	Eu, Tb, Y
	LEDs	Ce, Y
	LCD Backlights	Eu, Tb, Y
	Plasma screens	Eu, Tb, Y
	Cathode-ray tubes	Eu, Y
	Others (specialty)	Also Tm
	Automobiles	
	Mobile phones, Hard disk drives, Computers	
	Consumer electric and electronic devices	
	Industrial applications	Medium Dy level
	Electric bicycles	Higher Dy level
	Electric vehicles and hybrid electric vehicle motor	Higher Fy level
	Wind turbine generators	
	Other applications from magnet	Sm
	Nickel metal hydride batteries	La, Ce, Nd, Pr
	Rechargeable batteries	
	Electric vehicle and hybrid electric vehicle batteries	
Landfilled REE containing	Industrial residues	all

### 1.3. RRE Extraction technologies

Different technologies can be used for the recovery of REE from mineral and wastes depending on the mineral nature and the REE content. From classical methods of beneficiation, there are also numerous outstanding extraction techniques such as ion exchange, precipitation, solvent extraction, photochemical separation and supercritical extraction among others.

#### Gravity separation

RE minerals are good candidates for gravity separation as they have relatively large specific gravities (4–7) and are typically associated with gangue material (primarily silicates) that is significantly less dense (Jordens et al (2013)). This method is commonly used in monazite beneficiation.

#### Magnetic separation

Magnetic separation techniques are a common separation step in RE mineral beneficiation to eliminate highly magnetic gangue, or to concentrate the desired paramagnetic REE bearing minerals such as monazite or xenotime (Jordens et al (2013)). Along with gravity separation, magnetic separators are instrumental to monazite beneficiation from beach sands. They are used to eliminate strongly magnetic minerals such as magnetite prior to more selective separation steps, and are also used to separate paramagnetic monazite from non-magnetic heavy mineral gangue material such as zircon and rutile.

### Electrostatic separation

Electrostatic separation is a beneficiation technique that exploits the differences in conductivity between different minerals to achieve separation, this technic is typically used when other processing techniques fails to suffice, and the reason is simple, the energy required to drive off the mineral moisture are noteworthy. Usually used to separate the monazite and xenotime from gangue minerals with similar specific gravities and magnetic properties, one example would be the separation between ilmenite and xenotime, both with similar magnetic properties, and this case, the only method available to use is electrostatic separation([Gupta and Krishnamurthy, 1992](#)).

### Froth flotation

A process of selectively separating hydrophobic and hydrophilic elements is commonly used to the beneficiation of RE due to fact that is possible to process a wide range of fine particle sizes and process can be tailored to the unique mineralogy of a given deposit.

### Photochemical separation

The photochemical separation consists basically in four steps: dissolution and complexation process where chloride forms of the REE bonds with either hydroxide or isopropyl, photo-excitation where RE pass of its protons to chloride, electronics transition and precipitation. This technics is principally used for separation of different RE from each other. ([Alguacil et al. 1997](#), studied the separation of Eu (II) from a solution containing Sm and Gd:

- a) Dissolution and complexation process  
 $(\text{Sm, Eu, Gd})\text{Cl}_3 \cdot n\text{H}_2\text{O} + 3\text{EtOH} \rightarrow (\text{Sm, Eu, Gd}) \text{Cl}_3 \cdot 3\text{EtOH} + n\text{H}_2\text{O}$   
 $(\text{Sm, Eu, Gd})\text{Cl}_3 \cdot n\text{H}_2\text{O} + 3(\text{isoprop}) \rightarrow (\text{Sm, Eu, Gd}) \text{Cl}_3 \cdot 3(\text{isoprop}) + n\text{H}_2\text{O}$
- b) photo-excitation  
 $(\text{Sm, Eu, Gd}) \text{Cl}_3 \cdot 3\text{EtOH} \rightarrow (\text{Sm, Eu, Gd}) \text{Cl}_3 \cdot 3\text{EtOH}$   
 $(\text{Sm, Eu, Gd}) \text{Cl}_3 \cdot 3(\text{isoprop}) \rightarrow (\text{Sm, Eu, Gd}) \text{Cl}_3 \cdot 3(\text{isoprop})$
- c) Electronic transition  
 $\text{Eu} \cdot \text{Cl}_3 \cdot 3\text{EtOH} \rightarrow \text{EuCl}_2 + 2\text{EtOH} + \text{others}$   
 $\text{Eu} \cdot \text{Cl}_3 \cdot 3(\text{isoprop}) \rightarrow \text{EuCl}_2 + 2(\text{isoprop}) + \text{others}$
- d) Precipitation  
EuCl<sub>3</sub> is separated from the other rare earths

### Solvent extraction

Solvent extraction, consist in separating the REE in the leachate into different currents like light REE (La, Ce, Pr and Nd), medium REE (Sm, Eu and Gd) and heavy REE (Tb, Dy, Ho, Er, Th, Yb, Lu and Y) and after separate each of them into different currents ([Xie et al \(2014\)](#)). There are three major class of solvent extraction reagents: cation exchangers, solvation reagents and anion exchangers. In solvent extraction there are two important terms to be noticed, the distribution coefficient of a metal ion "M" named  $D_M$  and the separation factor of two different metal ions " $M_1$ ", " $M_2$ "  $\beta_{M1}$  and  $\beta_{M2}$ . Those two terms are given respectively by eq 1 and eq 2:

$$D_M = \frac{[\bar{M}]}{[M]} \quad \text{Equation (1)}$$

$$\beta_{M1/M2} = \frac{D_{M1}}{D_{M2}} \quad \text{Equation (2)}$$

Where  $[\bar{M}]$  is the molar concentration of metal M in the organic phase and  $[M]$  is the concentration in the aqueous phase, and as can see in the equation, the division between distribution coefficients of two different metals is the separation factor.

#### *a) Liquid cation exchangers*

Also known as acidic extractants, are one of three major classes of reagents for REE extraction from aqueous media as described by eq (3) ([Peppard et al., 1958](#)):



The M represents any REE and A denotes the organic anion, generally the process is more complicated than shown in eq. 3, a more accurate version of the process could be defined by eq 4 ([Mason et al., 1978](#)):



In this case the  $H_2A_2$  is the dimeric form of the organic acid. It can be noted that increasing the aqueous phase pH, the extraction is promoted, while decreasing its pH would in fact favor the stripping of the metal. Two main type of cation exchangers are used for the extraction of REE: carboxylic acids and organophosphorus acids.

- **Carboxylic acids**

Numerous studies has confirmed the usage of different carboxylic acids for the extraction of RRE. Naphthenic acid has been used for the separation of Y from lanthanides in China ([Li et al., 1994](#)) or sec-nonylphenoxy acetic acid and sec-octylphenoxy acetic acids, developed in China as an upgrade form of naphthenic acid have been used for the extraction of Y ([Wang et al., 2002](#); [Li et al., 2007a](#); [Li et al., 2007b](#); [Li et al., 2007c](#)).

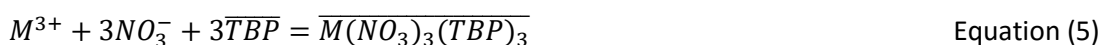
- **Organophosphorus acids**

Organophosphorus acids extractants are commonly used for the REE separation processes: D2EHPA (di-(2-ethylhexyl) phosphoric acid) and HEHEHP (2-ethylhexyl phosphonic acid mono-2-ethylhexyl

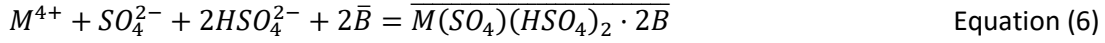
#### *b) Solvating extractants*

Numerous solvating agents have been used however TBP (Tributylphosphate) has been the most used. RRE could be extracted from chloride and nitrate medium by TBP increases with the increase in atomic number ([Jha et al. \(2016\)](#)). The distribution coefficients were found to be much lower in chloride compared to nitrate media. Concentrated nitrate systems proved to be more promising for separating REE lighter than Sm while the heavier one could not be separated effectively.

REE in neutral nitrate complexes are coordinated by the phosphoryl group of TBP, by and overall reaction described by eq 5:



When the the extraction takes place in sulphate media , as described by [Lu et al. Lu, 1998](#)) for the extraction of Ce(IV) and Th (IV) with Cyanex 923 in n-hexane as the reaction could be described eq 6:



Where M represents the rare earth (either Ce or Th), and B denotes Cyanex 923.

([Li et al., 2007a,b,c](#)) studied the extraction of trivalent lanthanides and Y from nitrate medium with Cyanex 925 in heptane, the reaction involved is described by eq. 7:



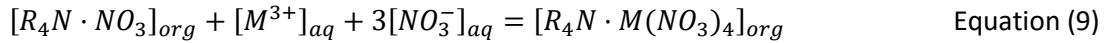
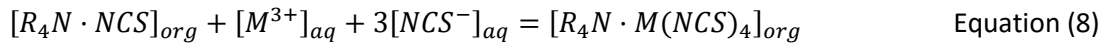
Where M represents lanthanides metal and B the Cyanex 925 extractant.

Recently, [Panda et al. \(Panda, 2014\)](#) studied the extraction of Pr using Cyanex 921 and Cyanex 923 from 0,008 M of nitric acid.

### c) Anion exchangers

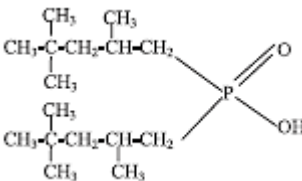
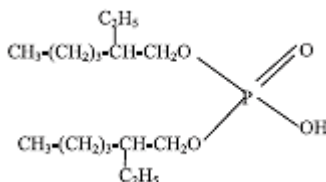
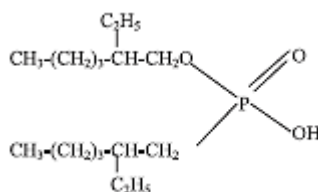
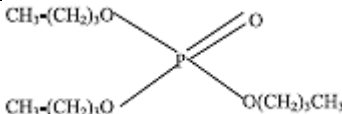
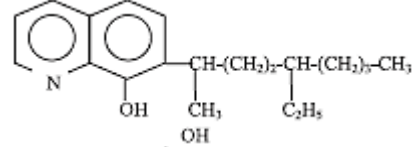
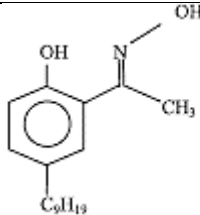
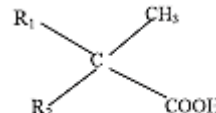
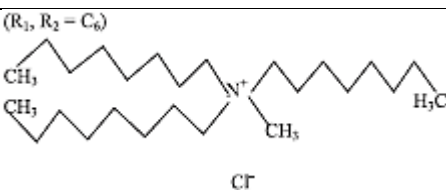
Anion exchangers extract metal ions as anionic complexes, and hence are only effective in the presence of strong anionic ligands. [Rice and Stone, 1962; and Bauer, 1966](#) shown that the separation factor for contiguous REE with primary or tertiary amines were unfavorable in chloride media, however it shows prospective in sulfate media.

The mechanism of the extraction has been studied by [Gupta and Krishnamurthy, 2005](#) as described by eq 8 and eq 9:



All the mentioned extractants are commonly used in industry nowadays and the different types can be seen in Table 10.

Table 10 Common commercially solvent extractas [Jha et al. 2016]

Solvent extractant	Extractants	Chemical name	structure
Cation exchanger  phosphorous acids	Cyanex 272	Di-2,4,4,-trimethylpentyl phosphinic acid	
	D2EHPA	Di-2-ethylhexyl phosphoric acid	
	PC 88A	2-Ethylhexyl phosphonic acid mono 2-ethylhexyl ester	
Solvating resin	TBP	Tri-n-butyl phosphate	
Chelating extractant	Kelex 100	7-(4-Ethyl-1-methyloctyl)-8-hydroxyquinoline	
Cation exchanger  Carboxylic acids	LIX 84	2-Hydroxy-5-nonylacetophenoneoxime BASF	
	Versatic 10	Alkyl monocarboxylic acids	
Anion exchanger	Aliquat 336	Tri-octyl methylammonium chloride	



## Ion exchange

Before 1960, ion exchange method was the only way to separate rare earth metals but currently it is used only to extract small quantities of highly purified rare earth products (Xie et al., 2014). Different ion exchange cationic or anionic resins are employed depending on the constituent of the aqueous solution using batch or continuous mode in column to extract Res from leached solutions with low RE concentration. The purified solution obtained after separation could be further processed to produce the value added products in the form of salt for industrial applications. Separation of rare earth metals by ion exchange process was initiated to separate fission products obtained from nuclear reactors (Spedding et al., 1956; Powell, 1961, 1964).

Chelating ion-exchange resins containing acidic functional groups, make the metal extraction process similar to the acidic extractants, but the resulting organic complexes are established by the organic anion coordinating the central cation in at least two position (Hudson, 1982). Urbanski et al., 1996; Arichi et al., 2006 examined the use of chelating resins for the extraction europium from nitrate solutions and cerium(III) and lanthanum(III) from chloride solutions, however the result was deemed to be less satisfactory in comparison with acidic extractant in Table 11, chelating resins used in this work are described.

Table 11 Common commercially ion extractant used in experiment (Jha et al. 2016)

Solvent extractant	Extractants	Chemical name	Structure
Chelating extractant	Cyanex TP207	Macroporous polystyrene crosslinked with iminodiacetic acid	$\text{RCH}_2\text{HN}^+ \begin{matrix} \nearrow \text{CH}_2\text{COOH} \\ \searrow \text{CH}_2\text{COOH} \end{matrix}$
	Purolite S957	Macroporous polystyrene crosslinked with divinylbenzene	

Just like the solvent extractant, the plentiful of chelating resin had also been tested for sake of extracting REE, in the Table 12, we can see a handful of example.

*Table 12 Salient results on extraction of rare earth metals using various extractant from different solutions*

Ion exchange process		
Resin used	Salient features	reference
Tulsion CH-96 and T-PAR	Solid-phase extraction of heavy rare-earths like Tb, Dy, Ho, Y, Er, Yb and Lu from phosphoric acid using Tulsion CH-96 and T-PAR resin has been reported.	<a href="#">Kumar et al. (2010)</a>
IR-120P (cation-exchanger polymeric resin)	Recovery of Y and rare earths using electroelution of a cation-exchange polymeric resin IR-120P Rohm & Haas-USA from chloride medium is reported.	<a href="#">Pinto and Martins (2001)</a>
N-methylimidazolium functionalized anion	N-methylimidazolium functionalized anion exchange resin was used for adsorption of Ce(IV) from nitric acid medium by reducing it to Ce(III).	<a href="#">Zhu and Chen (2011)</a>
exchange resin		
Tulsion CH-93	Solid-liquid extraction of Gd from phosphoric acid medium using amino phosphonic acid resin, Tulsion CH-93 is reported. The log D vs. equilibrium pH plot gave straight line with a slope of 1.8. The loading capacity of Tulsion CH-93 for Gd was 10.6 mg/g.	<a href="#">Radhika et al. (2012)</a>
D113-III resin	The adsorption and desorption behaviors of Er(III) ion using resin D113-III were investigated. The loading of Er(III) ion onto D113-III increased on increasing the initial concentration.	<a href="#">Xiong et al. (2009)</a>
D72 (acid ion exchange resin)	The loading of Pr (III) ions was dependent on pH and adsorption kinetics of Pr (III) ions onto D72 resin followed pseudo-second-order model. The maximum adsorption capacity of D72 for Pr (III) was evaluated to be 294 mg g <sup>-1</sup> for the Langmuir model at 298 K.	<a href="#">Xiong et al. (2012)</a>
D151 resin	The adsorption and desorption behaviors of Ce(III) on D151 resin was achieved at pH 6.50 in HAC–NaAc medium. The maximum loading capacity of Ce(III) was 392 mg/g resin at 298 K.	<a href="#">Yao (2010)</a>
TODGA resin	A two-stage method to separate Lu and Hf from silicate rock and mineral samples digested by flux melting or HF–HNO <sub>3</sub> dissolution using TODGA resin from Eichrom Industries is presented.	<a href="#">Connelly et al. (2006)</a>
Amberlite XAD-4	The pre-concentration and separation of La(III), Nd(III) and Sm(III) in synthetic solution was achieved using Amberlite XAD-4 with monoaza dibenzo 18-crown-6 ether. The adsorbed rare earth elements were eluted by 2MHCl.	<a href="#">Dave et al. (2010)</a>
D152 resin	The sorption of rare earth ions from HAC–NaAC buffer solution using D152 resin containing –COOH function groups at 298 K are presented.	<a href="#">Xiong et al. (2008)</a>
XAD-4 (crosslinked polystyrene resin)	A new chelating agent bis-2[(O-carbomethoxy)phenoxy]ethylamine has been synthesized using a facile microwave induced process. The ligand was appended on to XAD-4 resin and adsorption properties of La(III), Nd(III) and Sm(III) towards this resin were studied. The selectivity sequences of the resin for these metals were in agreement with their stability constants.	<a href="#">Kaur and Agrawal (2005)</a>
Tertiary pyridine resin	The novel separation method of rare earths using tertiary pyridine type resin with methanol and nitric acid mixed solution was developed. The adsorption and separation behaviors of rare earths were investigated and found that it can be well separated mutually.	<a href="#">Suzuki et al. (2006)</a>

## Supercritical extraction

Supercritical extraction consist in acquiring carbonate from of RE through a reaction from liquid suspension of REO with CO<sub>2</sub> with a temperature equal or higher than 31°C and 73 atm With this method, oxide form (RE (III)) and hydroxide form (of RE (IV)) can be obtained with 40°C and 100 atm. [Alguacil et al. 1997](#) claimed that the synthesis of the oxide forms of La, Nd, Sm, Eu, Gd, Dy and Ho is possible.

## Objectives of the study

The objectives of this study were the following

- To characterize the content of REE in two secondary resources: acid mine drainage waters and rich REE mining wastes from the remediation processes of acidic waters from the pyritic belt on Huelva.
- To identify suitable ion exchange resins to recover and concentrate REE from acidic waters.
- To quantify the influence of solution acidity on the extraction of REE and transition metals (TM).
- To characterize the metal extraction reactions involved.
- To determine the metal sorption capacities of the tested ion-exchange resins.

## 2. Experimental methodologies

### 2.1. Materials

Two ion-exchange resins were used: LEWATIT TP 207 (TP207) and Purolite S957 (S957) were used.

The TP 207 resin is a weakly acidic, macroporous cation exchange resin containing a chelating iminodiacetate group with good selectivity factors for transition metal cations from weakly acidic to weakly basic solutions. Divalent cations are removed from neutral waters in the order: Cu > V > U > Pb > Ni > Zn > Cd > Fe > Be > Mn > Ca > Mg > Sr > Ba >>> Na. The resin physical properties can be seen in the Table 13.

*Table 13 resin Lewatit TP 207 brochure*

Ionic form as shipped	Na <sup>+</sup>
Polymer structure	Macroporous crosslinked polystyrene
Appearance	Beige, opaque
Functional group	iminodiacetic acid
Total capacity (min.)	3,06 eq/l
Moisture retention	53-58%(H <sup>+</sup> form)
<425µm(max.)	5%
Uniformity coefficient (max.)	1.7
Specific gravity	1.1
Shipping weight (approx.)	720 g/l

The resin Purolite S957 is a chelating resin, which incorporates phosphonic, and sulfonic functional groups on a mechanically and osmotically resistant matrix. These combined properties give it high selectivity for iron and other transitional metals, even in acidic solutions. Purolite S957 is specially designed for the selective removal of ferric iron from acidic solution. Its properties can be seen in the Table 14.

*Table 14 Properties of Purolite S957 resin*

Ionic form as shipped	H+
Polymer structure	Macroporous polystyrene crosslinked with divinylbenzene
Appearance	Spherical beads
Functional group	Phosphonic and sulfonic acid
Total capacity (min.)	1,27meq/g (min.)
Moisture retention	55-70%(H+ form)
<425µm(max.)	5%
Uniformity coefficient (max.)	1.4
Specific gravity	1.12
Shipping weight (approx.)	710-760 g/l

To avoid the changes of acidity in the experiments with for TP207 resin, the initial sodium form was converted to the acid form. A given amount of 100 g of LEWATIT 207 resin was equilibrated with 200 ml of 1M H<sub>2</sub>SO<sub>4</sub> acidity of the solution measure as -log[H<sup>+</sup>] does no longer varies, the -log[H<sup>+</sup>] must remain below 3. After that the protonated form of the TP 207 resin was dried on the oven at 50°C for more than 24h. In the case of S957, it was used as received in the acid form.

## **2.2. REE containing samples: acidic mine waters and calcium rich mine wastes**

### **Recovery of REE from acidic mine waters.**

Acidic mine drainage (AMD) systems are generated by the dissolution of Fe sulfides as generate acidic solutions with pH values below 2. The dissolution rate of aluminosilicates increases with the catalytic action of H<sup>+</sup> ([Bloom and Stilling, 1995](#)), and, therefore, dissolution of rocks and the release of solutes to the pore water are much more intense in AMD environments than in the rest of weathering profiles. Once in solution, REE are mostly complexed REESO<sub>4</sub><sup>+</sup>, as sulphate is the dominant complex ion in AMD waters (Figure 4).

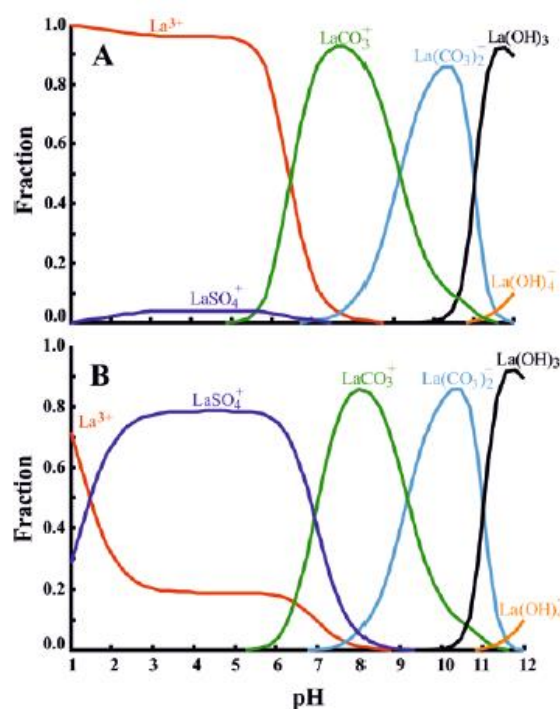


Figure 4 Variation of the relative abundance of  $\text{La}^{3+}$  aqueous species with pH in: A) pore water of a regular weathering profile ( $[\text{Total Inorganic Carbon}] = 1 \text{ mM}$ ;  $[\text{SO}_4] = 0.01 \text{ mM}$ ); B) acid mine water ( $[\text{Total Inorganic Carbon}] = 0.01 \text{ mM}$ ;  $[\text{SO}_4] = 1 \text{ mM}$ ). Thermodynamic data from MEDUSA database (Puig-Domenech, 2010).

Sulfate complexation inhibits the sorption of REE in clays and stabilizes them in the solution. As a consequence of the intense rock attack and the formation of stable complexes in solution, AMD contain REE concentrations much higher than other natural waters. Over one hundred of acid mine drainage have been described in Odiel and Tinto basins, and they are mainly discharges from galleries and open pits, and leachates from wastes. Some previous studies (Sanchez-España et al., 2005; Sarmiento, 2006) proved the existence of REE. Samples of AMD from two different mines (Poderosa Vella and Poderosa Nova) were collected by researchers of the Geochemistry research group of IDEEA (CSIIC) and analyzed by ICP-OES and ICP-MS.

In figure 5, it is shown the location of the different mines at the Tinto and Odiel basins.

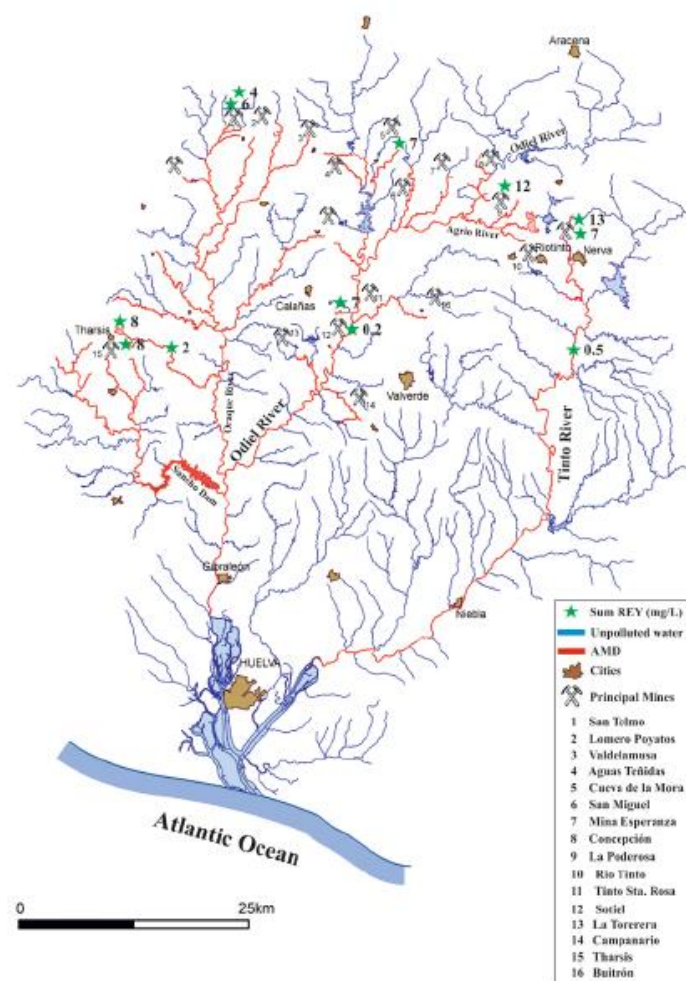


Figure 5 Location of mines in the Tinto and Odiel basins (SW Spain).

### Recovery of REE from solid mining wastes from on-site acid mine treatment on Odiel basin mines.

From the observations on REE behavior in rivers described above, it is expectable that an increase in pH above 5.5 will lead to the removal of REE from solution. Therefore, REE from acidic solutions can be accumulated in the precipitates of remediation systems once these pH values are reached. Recently ([Ayora et al, 2016](#)) developed a multi-stage sequential treatment of AMD using combination of neutralizing minerals as calcite and caustic magnesia. The experimental setup was based on a downward gravitational flow; it is made up of two successive columns filled with calcite (designing to precipitate trivalent metals, Figure 6-1) and caustic magnesia (for divalent metals precipitation, Figure 6-2), and decantation vessels. Once completed the experiment, samples of the newly-formed phases were obtained in both columns and the decantation vessel. Samples were analyzed for major and trace components, and their mineralogy were studied by X-Ray Diffraction and Scanning Electron Microscope (SEM) and Energy Dispersive Spectrometry (EDS). From these column the sections where Al is precipitated, was characterized by the highest content of metals on the remediation material. These samples from column 1 (C12, C13, C14) and samples from column 3 (C37, C38, C39) were selected for waste solid samples for REE recovery.

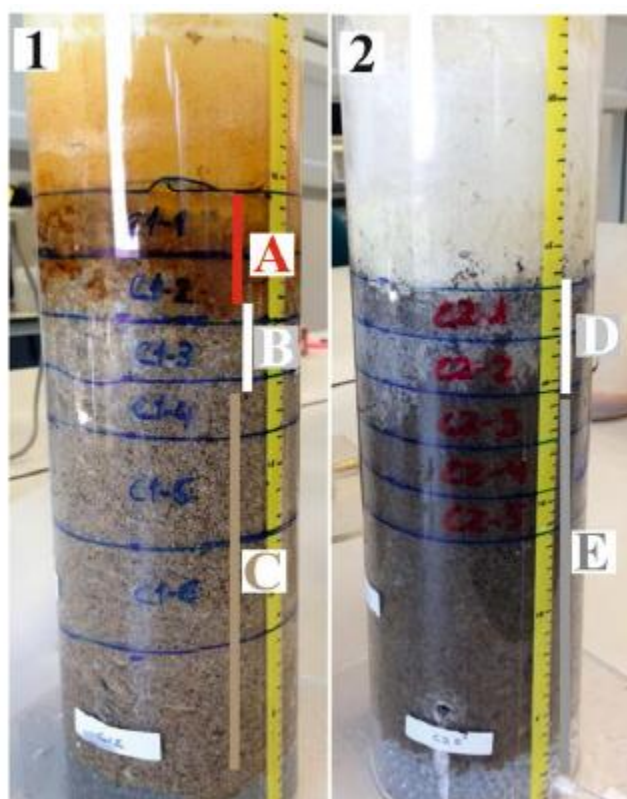


Figure 6 examples of columns treatment after 4 month of AMD percolation. 1) Calcite-DAS column showing three zones: a red zone of schwertmannite (A), a white zone of basaluminite (B), and a creamy zone of gypsum and unreacted calcite (C). 2) MgO-DAS column showing a white zone of gypsum and Zn-hydroxides (D) and unreacted MgO (E) (reference)

Samples from the column between 0.2 to 0.3 grams were dissolved with the minimum amount of HCl (11 M) and H<sub>2</sub>SO<sub>4</sub> (18 M) using batch experiments. Samples were equilibrated for more than 24 hours and after were filtered. Aqueous solutions were measured by Inductively Coupled Plasma Mass Spectrometry (ICP-MS).

### Analysis methodologies

Determination of Ce and La by spectrophotometry ([Castro 2015](#)) using arsenazo (III) as complexing ligand. For La (III) samples were 0.5, 4, 8, 12, 16 and 20 ppm and as for Ce (III) the samples were 1, 5, 10, 15 and 20 ppm were prepared from a 1g/L La (III) and 1.0 g/L Ce (III) standard solutions respectively by proper dilution.

Acid mine drainage samples from two different mines were received (mine Poderosa Vella and Poderosa Nova).



## 2.3. Metals extraction methodologies

### Determination of the equilibration time

Solutions of 250 mL with 25 mg/L of REE were prepared and 2 g of ion exchange resins were added in the solution and left in agitation with 250 rpm for 24 h. Samples of 3 mL were taken at given times [1, 5, 10, 15, 30, 60, 120, 240, 480, 1440] min.

### Effect of $-\log [H^+]$ on REE and transition metal extraction

Four single experiments were carried out using Ce (III) and La (III) as model REE with both resins. Seven samples were prepared for each experiment, each sample has different acidity ( $-\log [H^+]$ , between 2 and -1,5). Each sample of 25 mL contained either 20 ppm of La (III) or 20 ppm of Ce (III) and different amounts of  $H_2SO_4$  in order to achieve the required  $-\log [H^+]$ . Samples were left in agitation at 300 rpm for 24 h to reach the equilibrium by using a Heidolph REAX2 agitator.

Also Zn, Cu, Fe and Cd were used as model transition metal for model experiments. For the transition metal extraction, the samples have a volume of 50 mL and were prepared with 20 ppm of Zn, Cu, Fe or Cd. In each sample, 0,2 g or 2 g of either TP 207 or S957 resins were added. For each resin seven samples were prepared, each sample with different acidity ( $-\log [H^+]$ : 1, 1.5, 2, 2.5, 3 and 4). The samples were left in agitation to achieve the equilibrium.

### Effect of mass of resin on REE and transition metals extraction

The samples for these experiments were prepared by adding directly acid mine drainage from Huelva and then fix the acidity to pH 2.3. Each sample has a volume of 25 mL and in each of them different amount of either resin TP207 or resin S957 was added in order to study the effect that resin dose would have in the extraction of REE. However due to the fact that the acidic waters also contain transition metals, their extraction was also carried out. For both resins, four different amounts of resins were used (e.g. 0.5, 1, 2 and 5 g) and then the samples were left in agitation in Heidolph REAX2 until equilibrium was reached.

### Separation of REE from transition metals

The experiment was carried-out in two steps. The extraction ratio of REE and TM in synthetic water and the extraction of same metal with real acid mine drainage from Huelva. The samples used for the experiment using synthetic water were prepared with 3 ppm of each REE: Y, La, Ce, Pr, Nd, Sm, Gd, Dy and Yb and 3 ppm of TM: Al, Mn, Cu, Zn, Co, Ca, Mg and Fe. Each sample has a volume of 25 mL and has added either  $H_2SO_4$  or HCl to achieve the different acidity ( $-\log [H^+]$ ) required.

The second step of the experiment, the separation of REE from TM from ADM, the samples were prepared from the AMD waters by adding  $H_2SO_4$  or HCl.

### Resin Saturation assays

Samples of S957 were prepared by adding in 100 mL of AMD in sulfuric acid to achieve 1 M  $H^+$ , then 5 g of S957 resin was added to one of the three solutions and left in agitation with 300 rpm during 24 h, taking samples regularly. After 24 h the resins were separated by filtration and then the process was repeated again until the third cycle is completed. Samples of TP207 resins were prepared similarly and the acidity ( $-\log [H^+]$ ) was fixed to values of 1.



- **Metal extraction data treatment**

The extraction results were treated in two different ways, on the one hand the extraction percent (Ex%) was calculated using equation (10) and on the other hand the resin metal sorption capacity ( $Q_t$ ) was calculated by equation (11).

$$E(\%) = \frac{C_0 - C(t)}{C_0} \times 100 \quad \text{Equation (10)}$$

$$Q_t = \frac{(C_0 - C(t))}{m} * V \quad \text{Equation (11)}$$

Where  $C_0$  represent the initial REE concentration in solution,  $C(t)$  the concentration at a given  $t$ ,  $m$  the mass of resin in grams and  $V$  the volume of solution in L.

### 3. Results and discussion

#### 3.1. Characterization of secondary resources samples:

##### 3.1.1. Acid mine drainage samples characterization

The acid mine drainage from two different sampling points of the Poderosa Mine (Bella and Nova) were analyzed by ICP-OES and ICP-MS and results are plotted in Figure 4. In both cases, the most notable TMs are Cu and Zn, with some remarkable difference Mn and Co, while the other TM concentration is too low to be considered as significant in comparison with the majors.

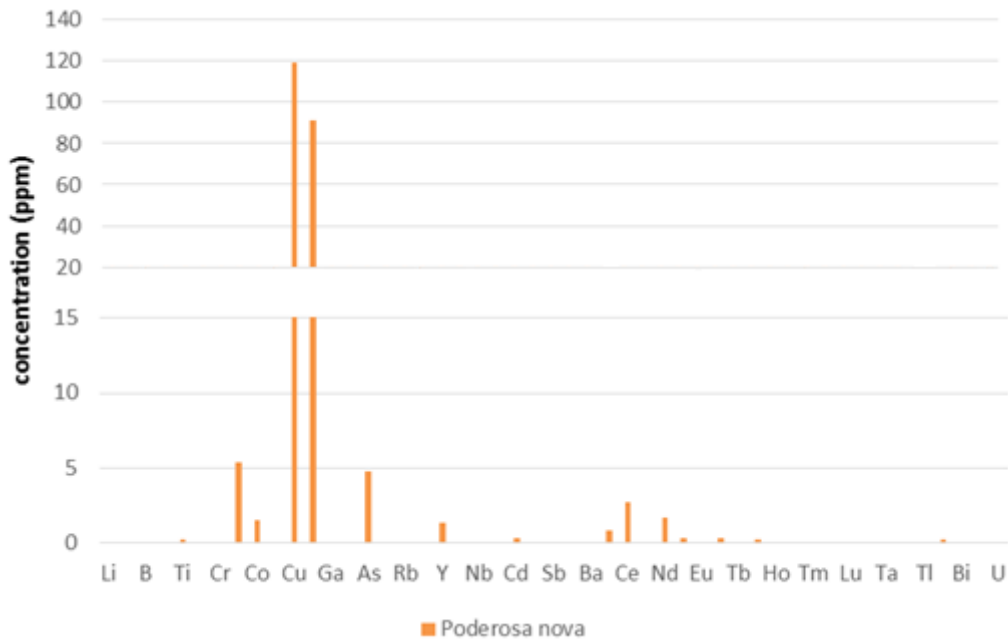


Figure 7 Transition metal in AMD from Poderosa Nova mine

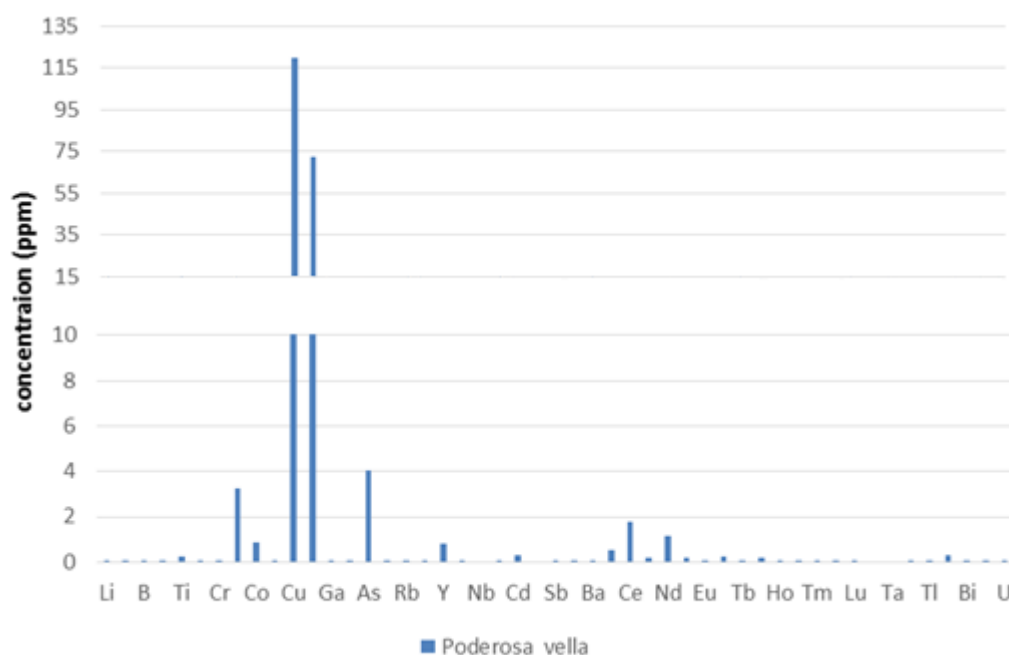


Figure 8 Transition metal in AMD from Poderosa Vella mine

It is found that REE are present in the acid mine drainage, at lower concentration ranges (in the mg/L) and between them the most abundant REE are Cerium, followed by Neodymium, Yttrium and then Lanthanum. The rest of them, although present, their concentration is too low, to be considered as significant. On the other hand, it is also important to notice that the concentration of REE in AMD from Poderosa Nova appear to be higher Over one hundred of acid mine drainage have been described in Odiel and Tinto basins, and they are mainly discharges from galleries and open pits, and leachates from wastes. In most of the monitoring studies ([Sanchez-España et al., 2005](#); [Sarmiento, 2006](#)) have proved the existence of rare earths elements with similar values to those measured in this study.

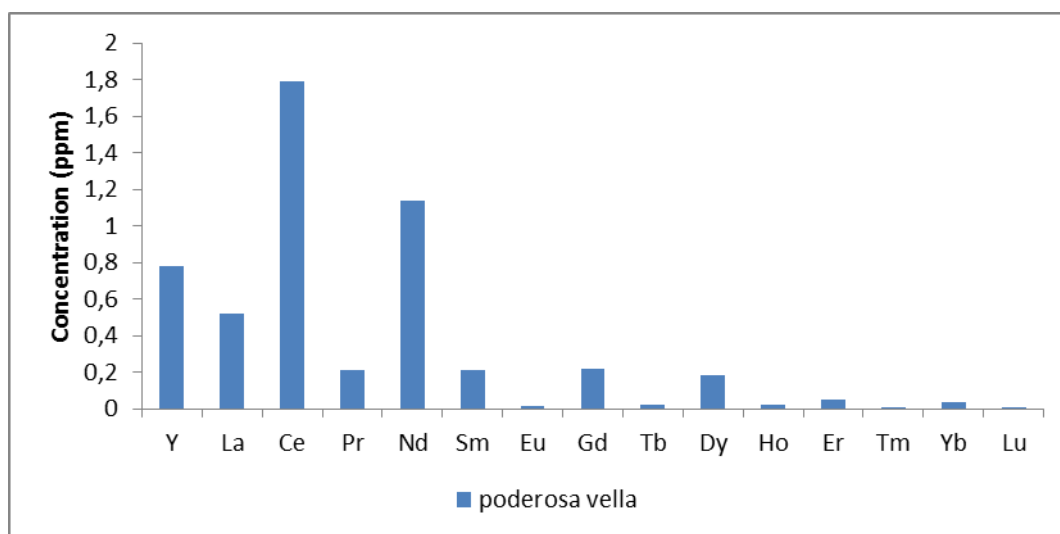


Figure 9 REE in AMD from Poderosa Vella mine

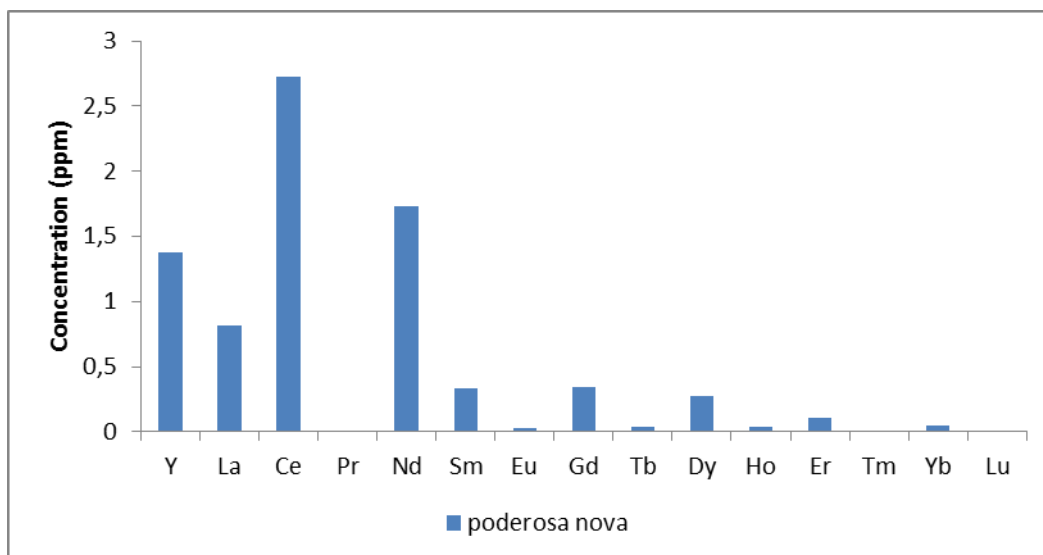


Figure 10 REE in AMD from Poderosa Nova mine

### 3.1.2. Analysis of solid wastes generated during the neutralization of AMD with basic amendments using column experiments.

Samples from laboratory column experiments with calcite (designed to precipitate trivalent metals, Figure 6-1) and caustic magnesia (for divalent metals precipitation, Figure 6-2), at different column lengths were selected. Those selected according to the highest content of RRE associated with the precipitation of basalaluminate were analyzed by ICP-MS and ICP-OES after total digestion and the results on transition metals and REE concentrations on mg metal/g solid waste are collected in table 15-19.

Table 15 Concentration of transition metal in solid samples C1-2 to C1-4

(mg/g)	Al	B	Ca	Cu	Fe	K	Mg	Mn	Na	Ni	S	Si	Sr	Zn
C1-2	35,4	0,8	151	0,3	53	1,3	2,3	0,3	0,4	0,02	29	0,02	0,1	0,83
C1-3	38,1	0,6	213	0,3	2,4	0,3	2,6	0,2	0,4	0,03	1,8	0,01	0,1	1,26
C1-4	12,1	0,5	244	0,4	0,9	0,2	2,4	0,2	0,3	0,02	2,0	0,2	0,1	1,46

Table 16 Concentration of REE in solid samples C1-2 to C1-4

(mg/g)	Y	La	Ce	Pr	Nd	Sm	Eu	Gd	Tb	Dy	Ho	Er	Tm	Yb
C1-2	0,019	0,016	0,052	0,007	0,027	0,009	0,001	0,007	0,001	0,006	0,00	0,003	0,00	0,003
C1-3	0,024	0,026	0,085	0,011	0,044	0,013	0,002	0,010	0,001	0,007	0,001	0,003	0,00	0,003
C1-4	0,041	0,046	0,156	0,021	0,081	0,024	0,003	0,019	0,003	0,014	0,002	0,005	0,00	0,005

Table 17 Concentration of transition metal in solid samples C3-7 to C3-9

(mg/g)	Al	B	Ca	Cu	Fe	K	Mg	Mn	Na	Ni	P	S	Si	Sr	Zn
C3-7	29	0,24	170	3,6	4,7	0,5	2,23	0,28	0,15	0,02	0,09	22	0,08	0,10	1,2
C3-8	33	0,24	194	7,0	4,9	0,2	2,61	0,32	0,20	0,02	0,01	47	0,03	0,10	1,3
C3-9	29	0,33	161	8,4	5,4	0,1	2,11	0,32	0,18	0,03	0,01	44	0,15	0,08	1,4

Table 18 the concentration of REE in solid samples C3-7 to C3-9

(mg/g)	Y	La	Ce	Pr	Nd	Sm	Eu	Gd	Tb	Dy	Ho	Er	Tm	Yb
C3-7	0,005	0,004	0,014	0,002	0,009	0,002	<ld	0,002	<ld	0,001	<ld	<ld	<ld	<ld
C3-8	0,008	0,004	0,018	0,003	0,013	0,004	<ld	0,003	<ld	0,003	<ld	0,001	<ld	0,002
C3-9	0,009	0,004	0,018	0,003	0,014	0,004	<ld	0,004	<ld	0,003	<ld	0,002	<ld	0,002

As it could be seen values of transition metals ranged between 20-30 mg/g for the case of Al, Ca, Cu and Zn, and for the case of REE values ranged from 0,004-0,02mg/g.

The compositions of solid samples after leaching with strong acids (HCl and H<sub>2</sub>SO<sub>4</sub>) are shown in Figures 11 and 12. In general higher concentration values of REE were reached when using HCl and H<sub>2</sub>SO<sub>4</sub>, and could be associated to the highest solubility of RRE containing precipitates. Values of REE measure reached the highest values for Ce, and when compared to the typical values found in AMD, the expected concentration factor was not reached.

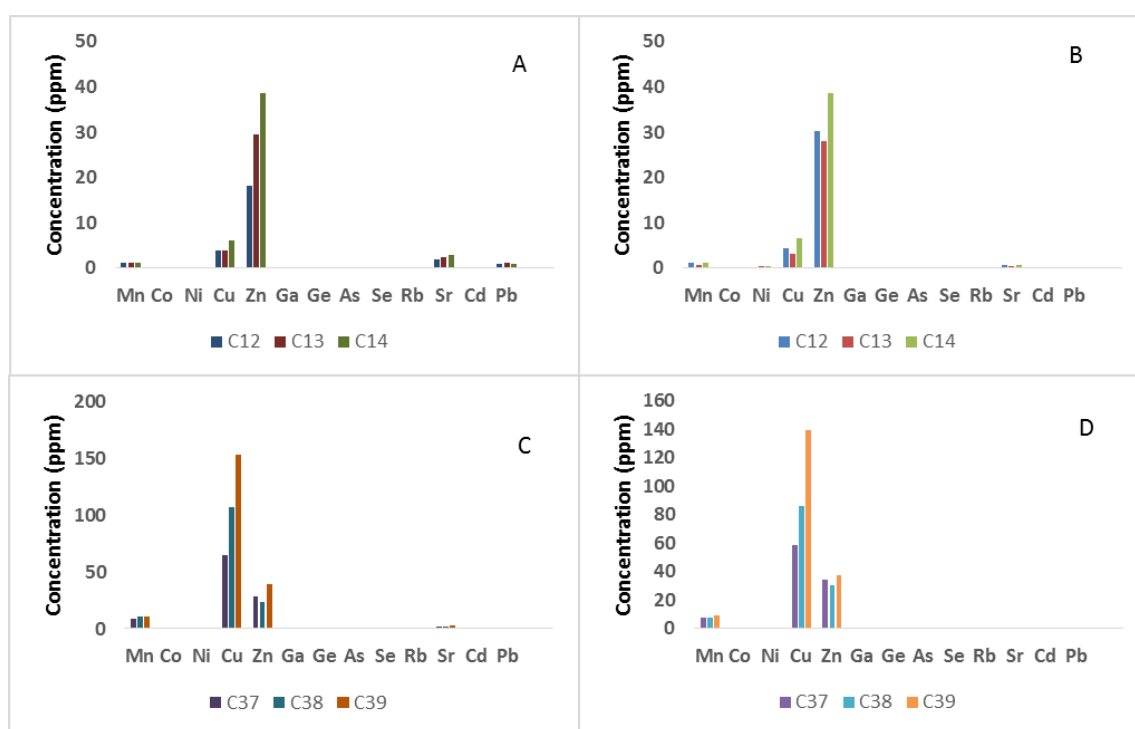


Figure 11 variation of transition metal in different samples leached with two different acids: in A and C, the samples are leached with 11M of HCl and B and D samples are leached with H<sub>2</sub>SO<sub>4</sub>.

From Figure 11, it can be observed that the predominant TM in the leachate is zinc and copper, with some “while significant, but pale in comparison” amount of manganese. In this situation the effect of the variation of acid dos not seems to be significant.

On the other hand figure 12 the rare earth concentration in the leachate varies with the deepness where the sample is taken and also the type of acid is used. Deeper the sample is taken, more concentrated is the leachate, however using HCl, the concentration is 3 to 4 higher in comparison with the solution leached with H<sub>2</sub>SO<sub>4</sub>.

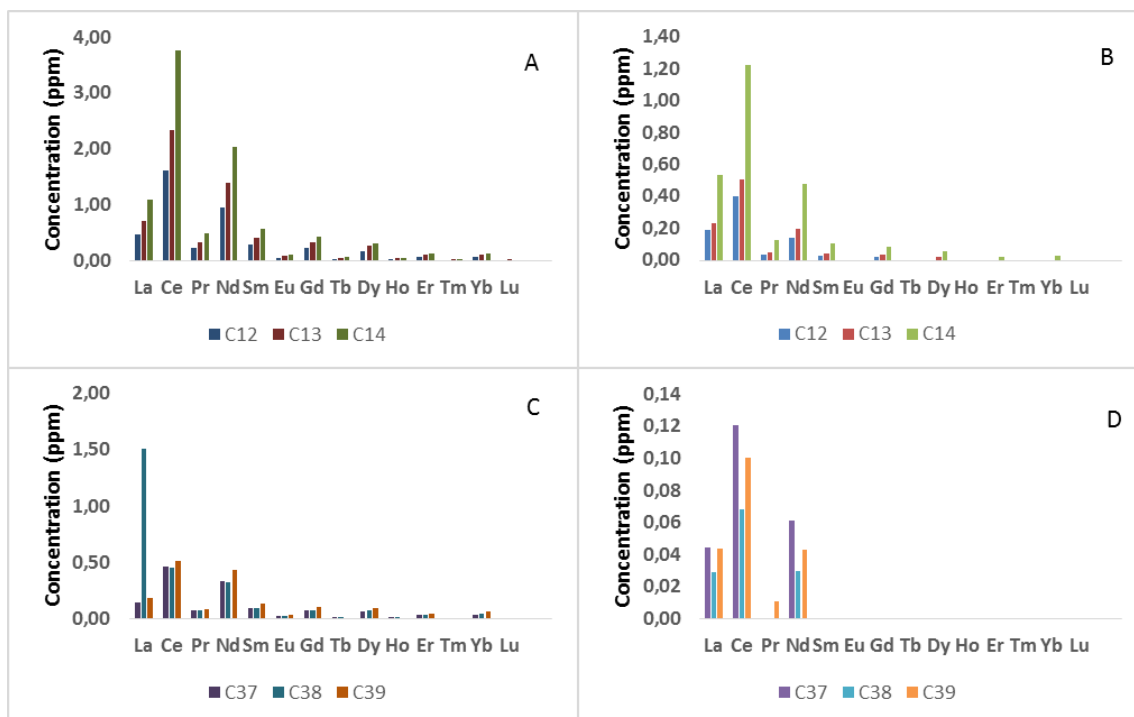


Figure 12 variation of REE in different samples leached with two different acids: A and C samples are leached with HCl while B and D samples are leached with H<sub>2</sub>SO<sub>4</sub>

Also not significant differences were found for both type of origins: column 1 with mixture of a disperse alkaline substrate of Calcite (Calcite-DAS) column and column 2 using a mixture of a disperse alkaline substrate with magnesium oxide (MgO-DAS)

### 3.2. Metal extraction kinetic with ion-exchange resins S957 and TP207

As can be seen in the figure 13, the Lanthanum extraction of resin TP 207 varies with time, and its maximum extraction is over 60%, after 180 minutes of contact time. On the other hand, the maximum extraction percentage of La of resin S957 is nearly 100%, and its only takes roughly 30 minutes. In figure 13, it can also appreciate the variation of the La sorption capacity with time for both resins. In the case of TP 207, at equilibrium attainment, a sorption capacity of 2 and 2.5 mg of La/g resin for S957. In case of Ce, a similar results were obtained. The maximum extraction achievable by TP 207 is slightly lower than 70 % and in comparison; the maximum extraction ratio attainable by S957 is almost 90%.

On the other hand, in Figure 14, slightly more than 3 mg of Ce is absorbed by each gram of S957 resin, while of each gram of TP 207 resin, only 2.5 mg of Ce was absorbed.

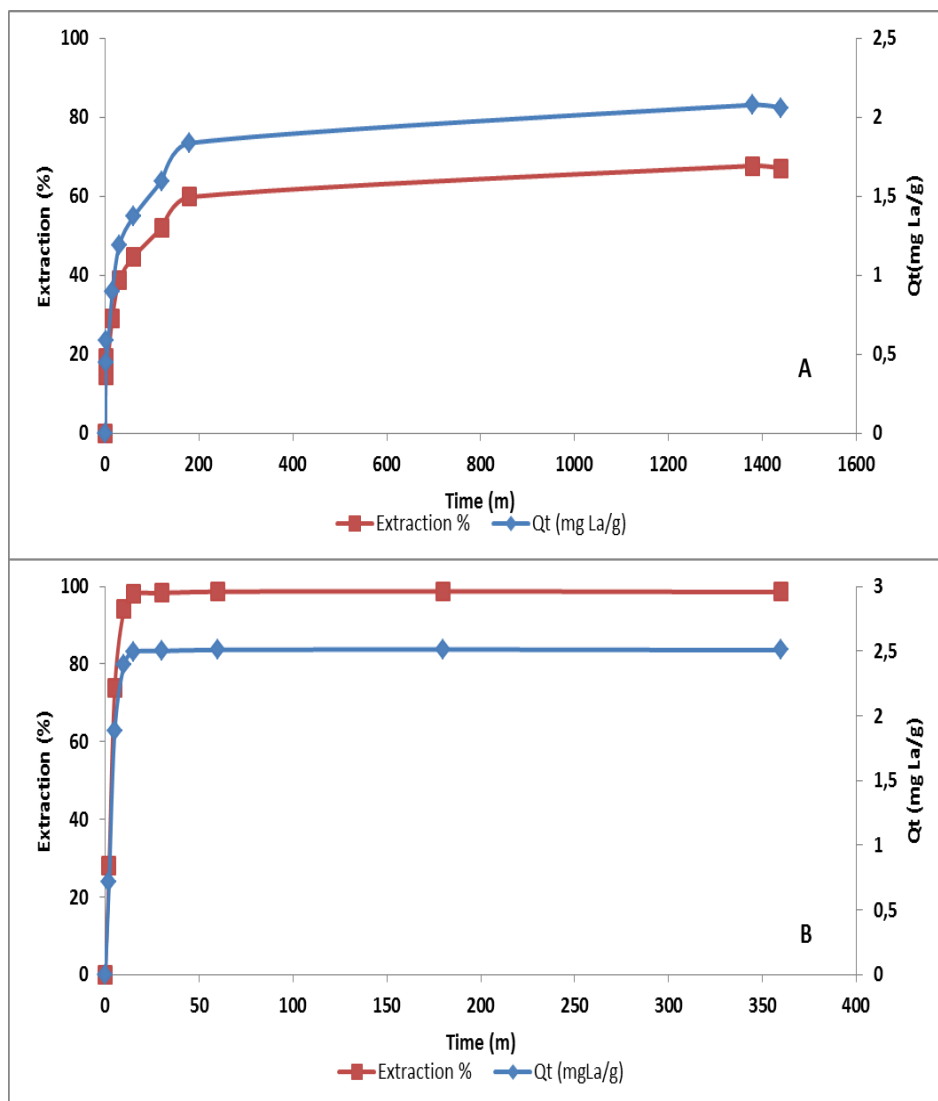


Figure 13 Kinetic absorption of La (III): A using TP 207 and B using S957

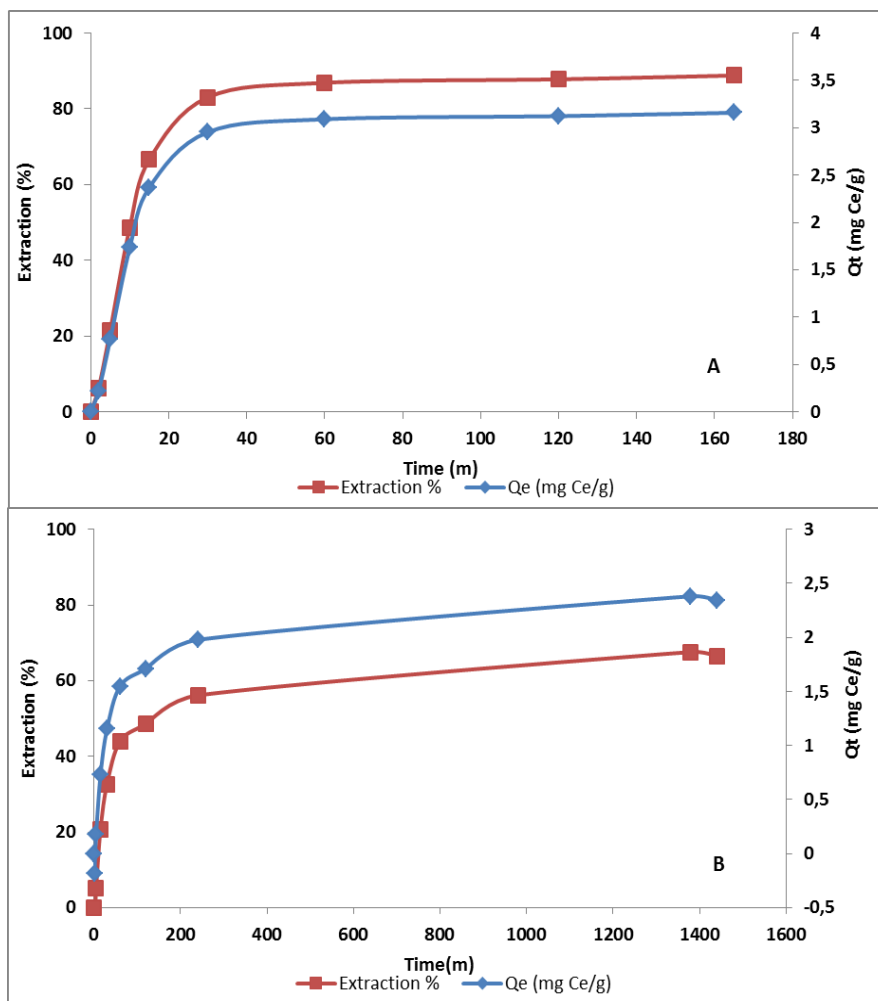


Figure 14 Ce kinetic performance using: A using S957 B using TP 207

### 3.3. Extraction dependence of REE on solution acidity

As can be seen in Figure 15, the extraction of Ce and La, is strongly affected by the acidity and in a different way depending on the resin properties (e.g. nature of the functional group). In case of Ce (III), TP207 resin has a strong decrease of extraction efficiency over  $-\log[H^+]$ , and for lower acidity the extraction remain same as the  $-\log[H^+]$  decreases, however for the S957 resin the decrease begins at  $-\log[H^+]$  of 0.5, and it is decreasing steadily until  $-\log[H^+]$  values of -1. S957 resin containing a two functional groups, a sulphonic group and and amoniphosphonic groups shows high metal efficiency that TP207

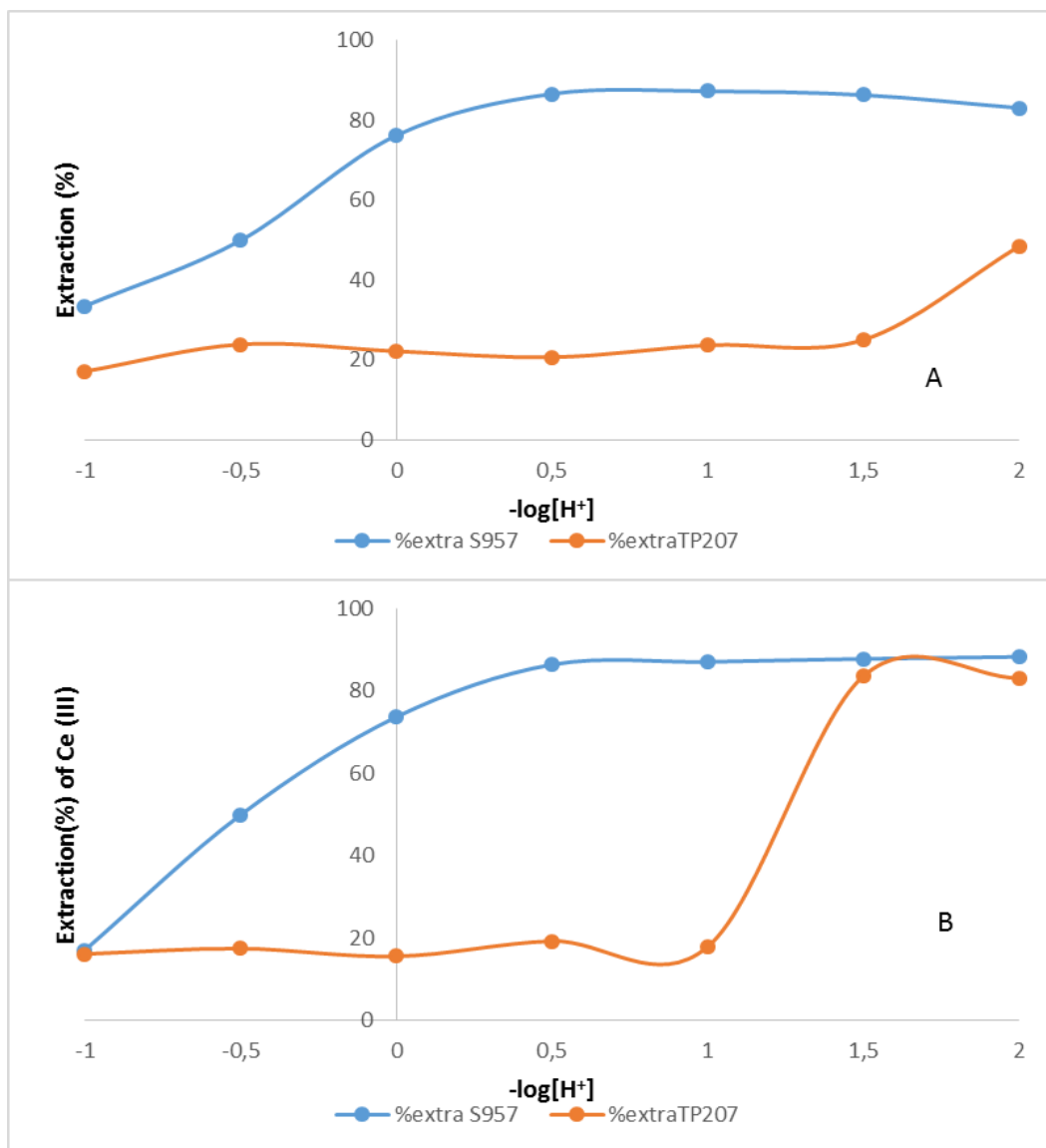


Figure 15 Effect of pH on extraction of REE: A La (III) and B Ce (III)

The extraction profiles of S957 are similar to those described in the literature when using acidic organophosphorus extractants ([Panda et al. 2014](#)). More limited data could be found for extractants carrying carboxylic groups, however even at very high acidity values the TP207 have shown extraction of Ce and La.

Results of transition metals (Cu, Zn and Fe) are shown in Figure 16. For S957 using 4g/L shown extraction ratio stables and maximum from  $-\log [H^+]$  2 to 4, however at higher acidities ( $-\log [H^+] < 2$ ) the extraction begin to decrease from  $-\log[H^+] < 2$  and a considerable difference in extraction is seen, especially with the case of Copper, whose extraction rate is only 10%, while for the others the extraction rate is over 50%.



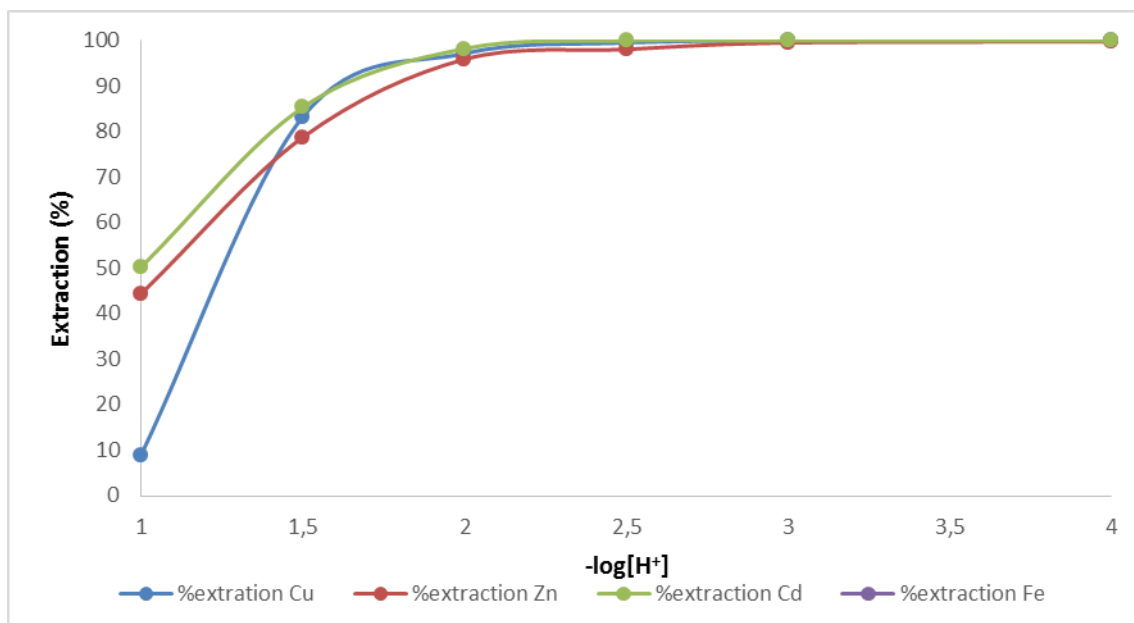


Figure 16 Extraction of transition metals as a function of pH for a 4g/L of S957 dose

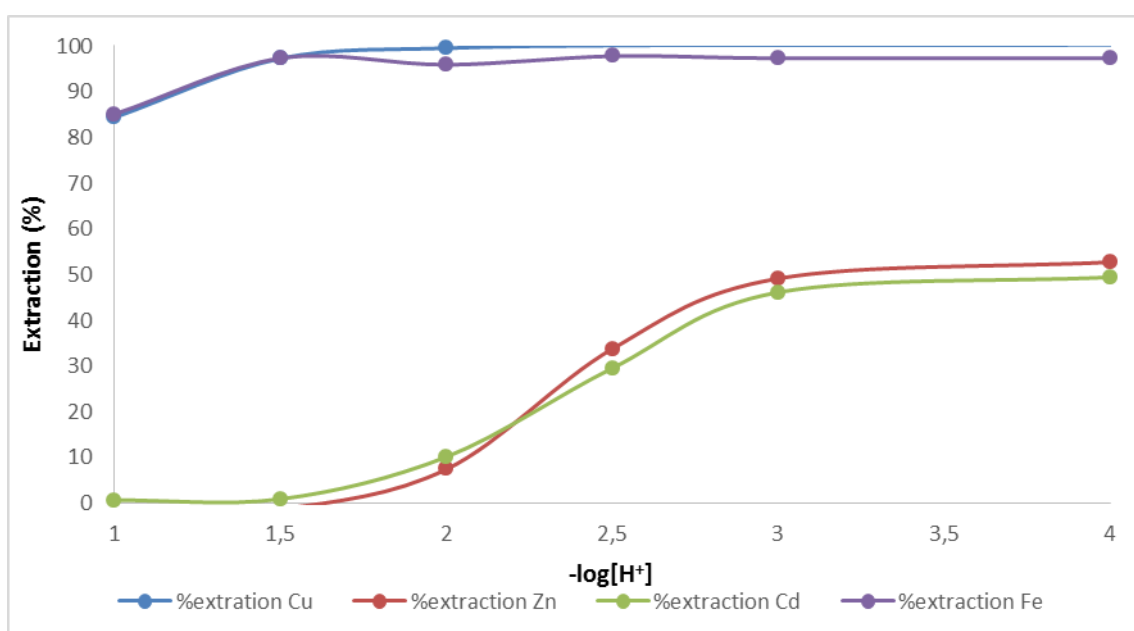


Figure 17 Extraction of transition metals as a function of pH for a 4g/L of TP 207 dose

When TP207 resin was used, (Figure 17) a different profile was seen between the different transition metals. While Fe and Cu (II) are extracted along with the acidity range evaluated, for Cd and Zn, the resin capacity is lost for acidities below  $-\log [H^+] 2$ . On other hand, the extraction ratio of Fe and Cu was kept around 100% along the acidity range evaluated.

When using 40g/L of S957 resin (Figure 18) the extraction ratio profiles change drastically. The selectivity shown for TP207 is lost and all four transition metals are extracted in the acidity range

evaluated, however Zn and Cd extraction ratios decrease close to zero for acidity values below  $-\log [H^+]$  of 1.

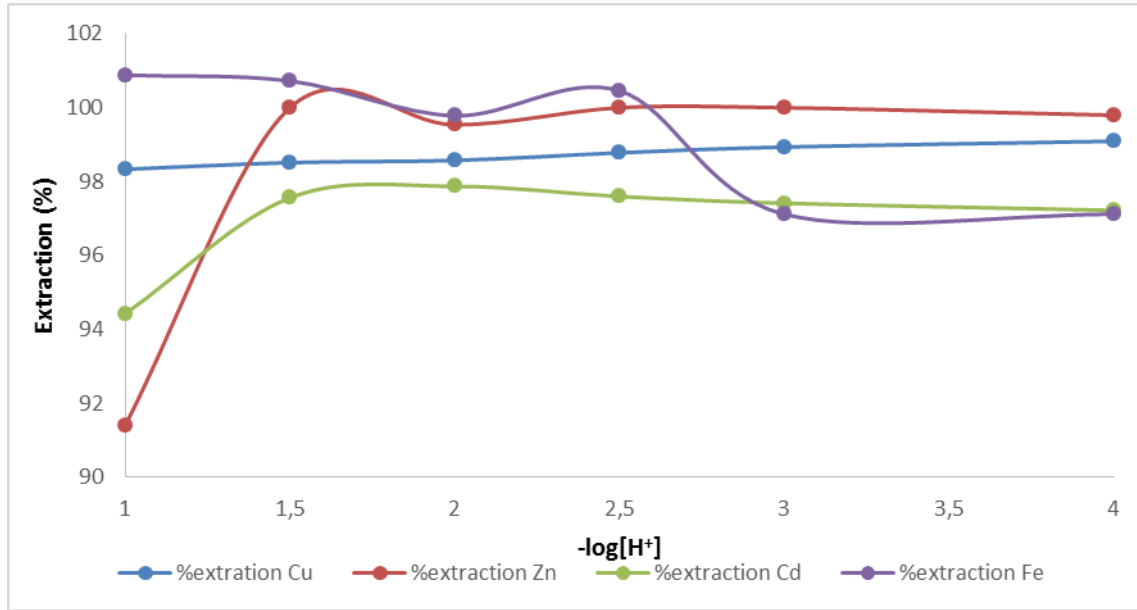
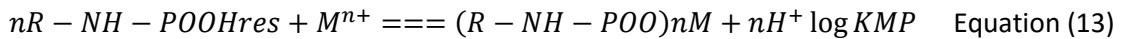
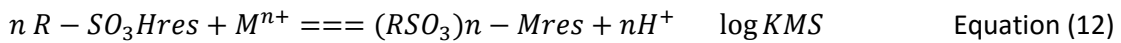


Figure 18 Extraction of transition metals as a function of solution acidity for S957 resins (phase ratio 40 g/L )

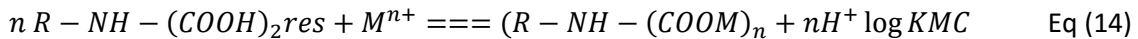
Both Fe and Cu remain at their maximum extraction ratio along the range of acidity.

The differences observed between resins are associated to the metal extraction reactions involved:

For resin S957 with two functional groups involved the metal extraction reactions to be considered will be:



For resin TP207 with an iminodiacetic group involved the metal extraction reactions defined will be:



The affinity of the exchanged ions for the cation exchanger depends majorly on the charge, size and degree of hydration of the exchanged ions while for ions with the same charge, the affinity depends on their size and degree of the hydration. As the atomic number of rare earth metals increases their ionic radius decreases and due to their similar values of ionic radius, there are no significant differences in their affinity for the polystyrene cation exchangers. As a result, individual rare earth metal could not be positively extracted from the solutions of mineral acids. However, solutions containing mineral acids with organic solvents can improve the rare earths separation as they are much harder sorbed on cation exchangers than using aqueous solutions of these acids (Starý, 1966). However, the mechanism of the processes involved in anion exchangers was much more complex and could not be explained clearly. Rare earth metals show

little tendency to form anionic complexes with simple inorganic ligands and are poorly absorbed on the anion exchangers from aqueous solutions of hydrochloric and nitric (V) acids.

The differences between the each functional groups and the each metals, provides different metal extraction ratios. The extraction profile of each metal will be defined by the strength of their metal-functional groups, and can be used to find the separation factors.

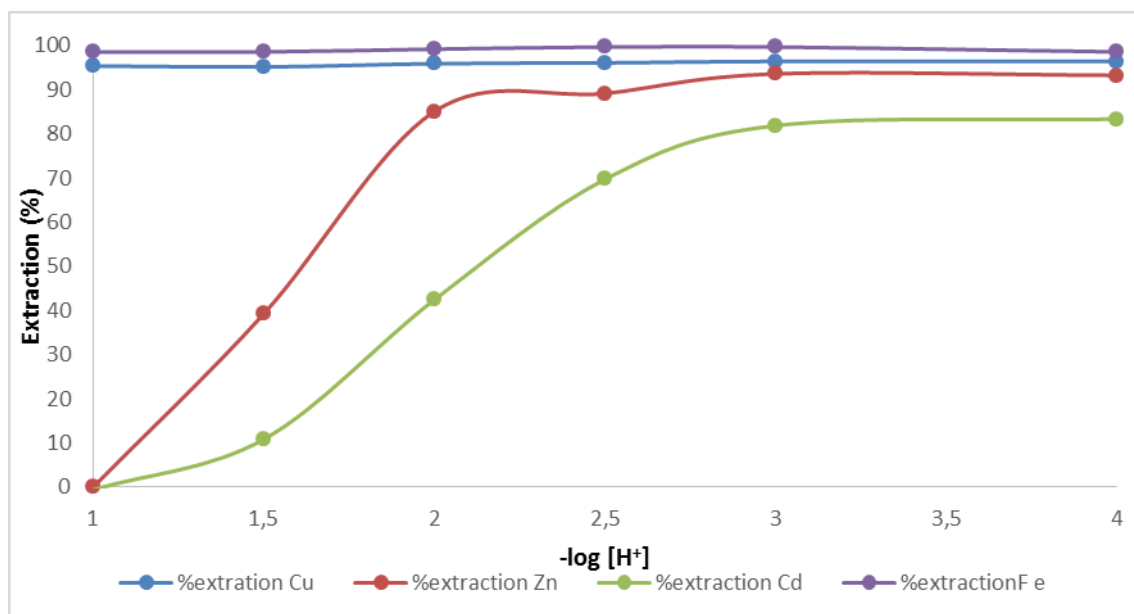


Figure 19 Extraction of transition metals as a function of solution acidity  $-\log [H^+]$  using 2g of TP 207

### 3.4. Evaluation of resin concentration on metal extraction reactions.

The influence of resin doses for both REE and TM extraction using the TP207 resin are described in Figures 20 and 21. When comparing the influence on the extraction patterns, they were more significant with TM than with REE with a few exceptions. The REE extraction in acid mine drainage with the exception of La, Ce and Gd, seems to remain unaffected with variation of the mass of resin TP 207. However when TM are analyzed, the variation seems to be taken with further importance, since extraction ratio of all transition metal seem to be affected.

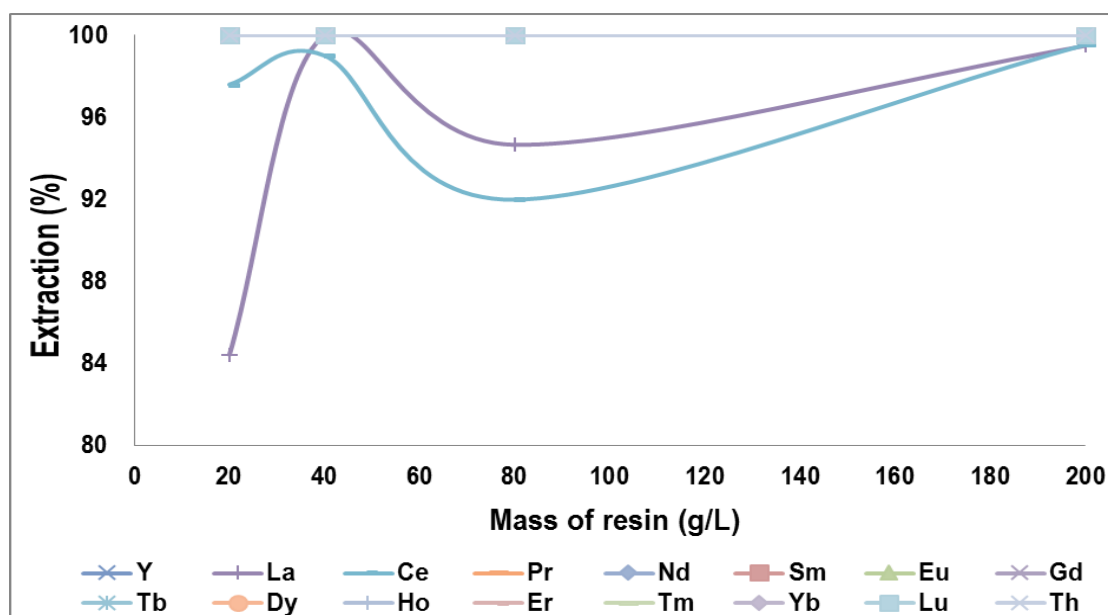


Figure 20 extraction of REE with different concentration of resin TP 207

With 200g/L of TP 207 resin, all transition metal have reached the full extraction, with 80g/L a slight diminution can be spotted with some of the transition metal. When 40g/L is used, a significant difference in extraction rate can be appreciated with Cu, Mn and Zn, however the rest remain the safe. With 20g/L of TP 207 used, the extraction rate of Cu, Mn and Zn, is downgraded to over 15%, while the other metal extraction ratio have shown sign of beginning to decrease.

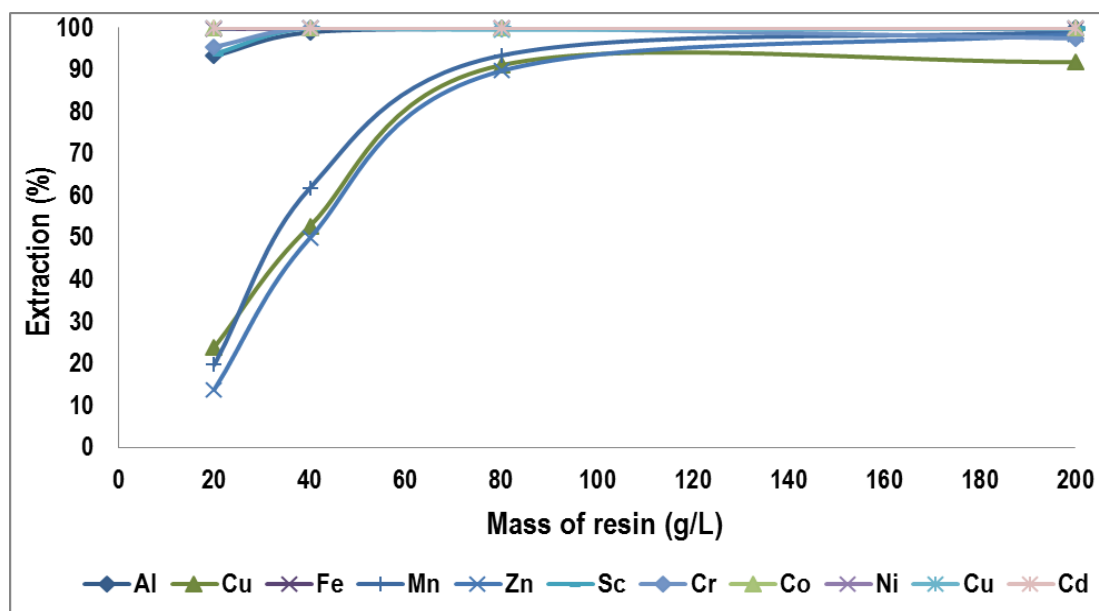


Figure 21 extraction of transition metal using different concentration of resin TP207

Similar scenario can be described for resin S957, in the extraction of REE, with some minor variation. As can be seen in Figure 22 and Figure 23, most of the REE have quantitative extraction for resin ratios higher than until the amount of the resin is 40g/L, at this moment, a reduction of the extraction ratio was measured, and with a 20g/L of resin, the extraction ratio of Dy is nearly 0, and for the rest a weighty difference can be seen.

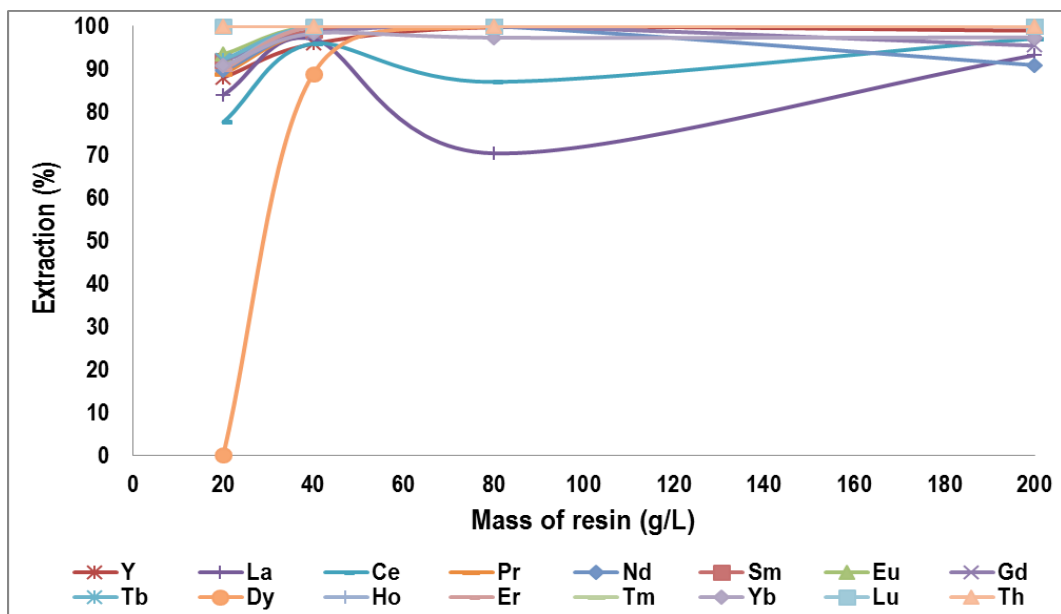


Figure 22 extraction of REE using variation of concentration of resin S957

With the extraction of TM, a quantitative extraction has been measured with 200g/L, except the case of Cr, whose maximum extraction is over 70%. Just like the extraction curve of the resin TP 207, the point where the extraction being to decrease is with 80g/L to 40g/L of resin, a significant difference can be seen in the curve of most of the TM, with some exception such as Fe, Cu, Sc, Zn and Mn. And for the final point with 20g/L of resin, the extraction of most TM is at its lowest values, the extraction percentage ranged between 10% and 30%. However some TM like Fe, Cu and Zn still remain at its maximum extraction ratio, while other such as Mn is just starting to decrease the concentration.

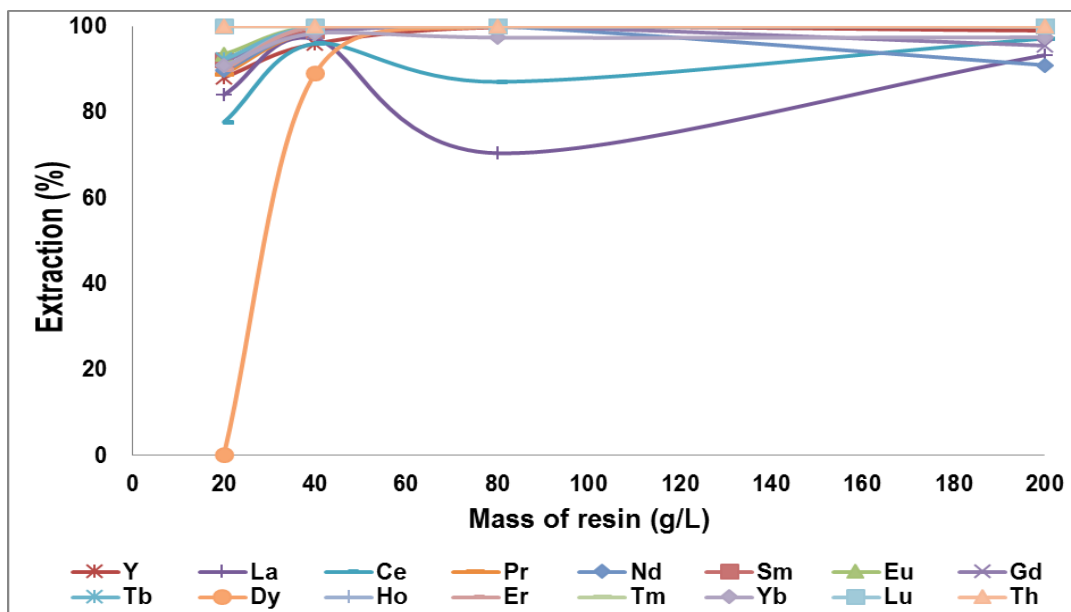


Figure 23 extraction of transition metal varying the concentration of S957 resin

### 3.5. Evaluation of the Separation factors of REE from transition metal

In Figure 24 it can be observed that using synthetic water resin S957 the maximum extraction of REE happens between  $-\log [H^+]$  0 and  $-\log [H^+]$  2 and it takes values of 100%. With  $-\log [H^+]$  lower than 0 the extraction ratio began to decline, and then with  $\log [H^+]$  -1, the extraction ratio varied between 37% (La (III)) and 56% (Sm and Gd).

With TM, a slight different scenario is presented, the maximum extraction takes place between  $-\log [H^+]$  0.5 and 2 with exception of Al and Fe whose limit is  $-\log [H^+]=0$ . TM extraction reaches its lowest value (16%) at  $-\log [H^+]$  -1. However extraction of Fe and Al is still high in comparison with other and it's very similar to REE behavior.

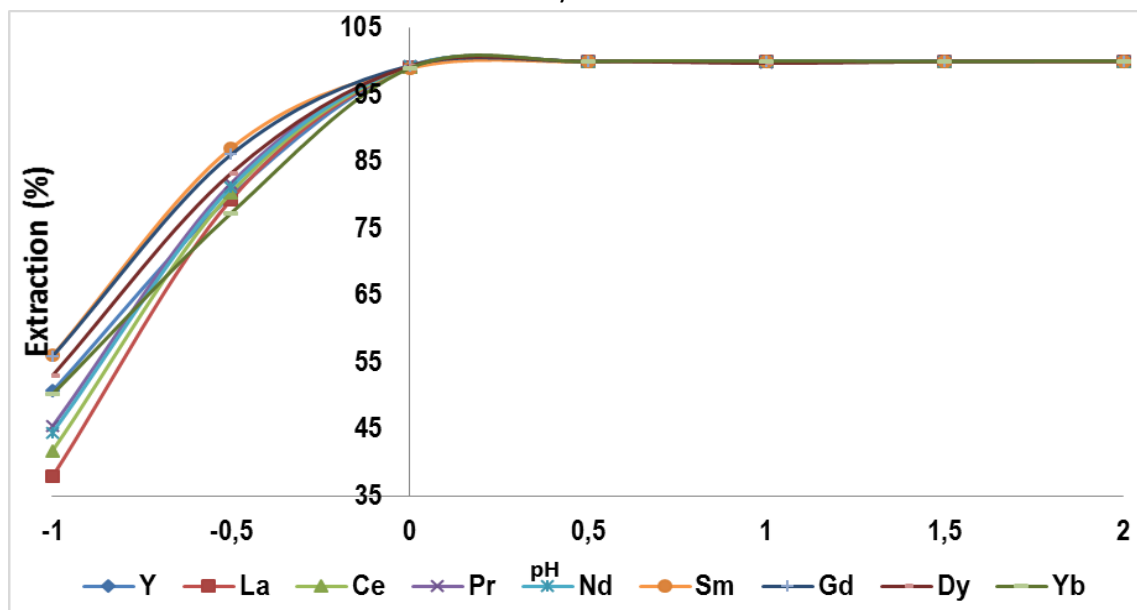


Figure 24 Extraction of REE in synthetic water with S957 in  $H_2SO_4$

For acid mine drainage solutions, the maximum extraction remain the same, however the effect that the  $-\log [H^+]$  had slightly changed. The extraction of REE began to decrease with  $\log [H^+]$  0.5 and it reached its minimum with  $-\log [H^+]$  -1, being Lanthanum the one with lowest extraction ratio(39%) and Gd and Sm the highest one (60%).

TR extraction had only small variations. The first one would that the maximum extraction is no longer 100% but between 80% and 90% except for Fe and Cu whose maximum extraction ratio remain the same.

Other feature to notice, is the fact that in this situation, Fe extraction is unaffected by the variation of the  $-\log [H^+]$ , and the extraction is at its maximum all the time.

If in place of using  $H_2SO_4$ , HCl is used, then a different extraction ratio of REE can be seen between  $-\log [H^+]$  -0.5 and -1, in this situation the extraction ratio of resin is compressed between 85% (Sm and Gd) and 75% (La and Ce) while with  $\log [H^+]$  higher than 0, the extraction seem to be same, as using  $H_2SO_4$ : 100%.

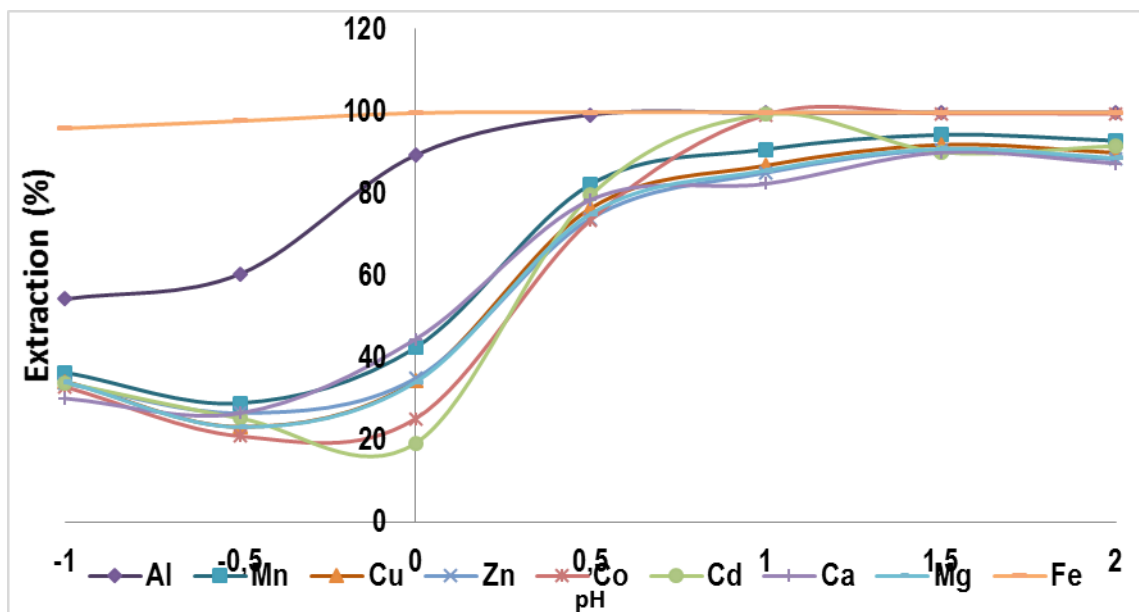


Figure 25 extraction of transition metal with S957 in AMD in  $H_2SO_4$

Similar behavior can be seen with extraction ratio of TM, only a small variation can be seen in comparison with the extraction with  $H_2SO_4$ . The extraction starts to decrease with  $-\log [H^+]$  between 0,5 and 0 (Fe and Al). After that the extraction remains stable between 40% and 60% with some exception such as Al and Fe.

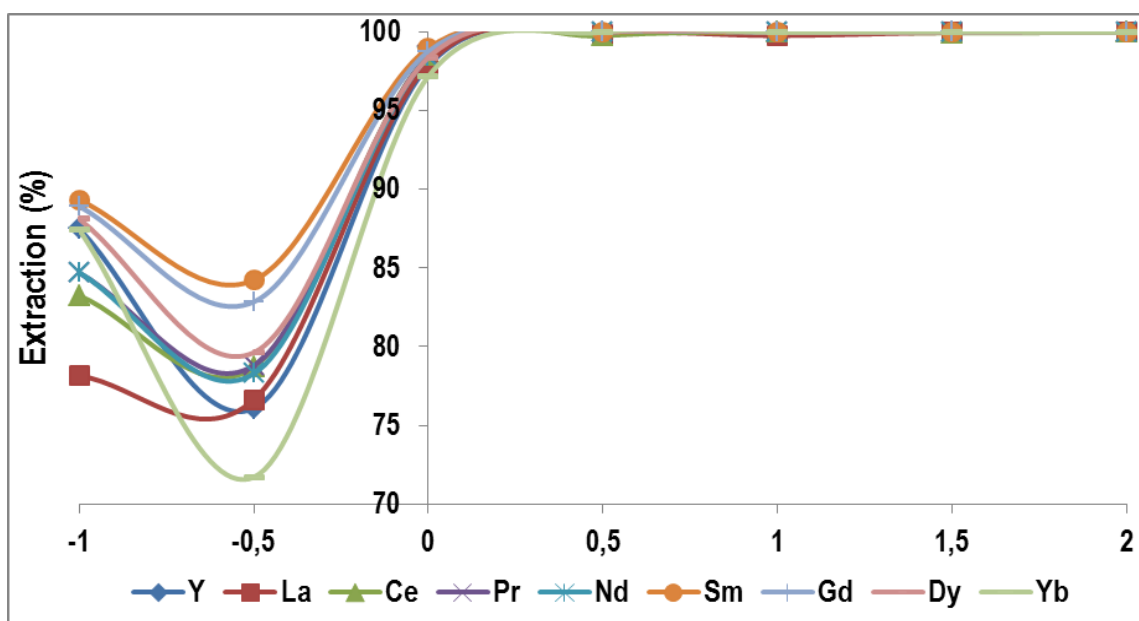


Figure 26 Extraction of REE within synthetic water with HCl with S957

When using then AMD from Odriel basin mines, the extraction of REE also began to drop in  $\log[H^+]$  0, reaching an extraction between 80% and 70% can be seen in  $-\log[H^+]$  -1, with exception of La, whose extraction is 40%.

When transition metal is involved, the extraction is fairly the same in comparison with one using  $\text{H}_2\text{SO}_4$ , the maximum extraction is between 80% and 60% with exception of Fe and Al, whose maximum extraction is 100%, all other metal start decreasing their extraction ratio at very beginning, reaching 30% of extraction by the  $-\log[\text{H}^+]$  -1.

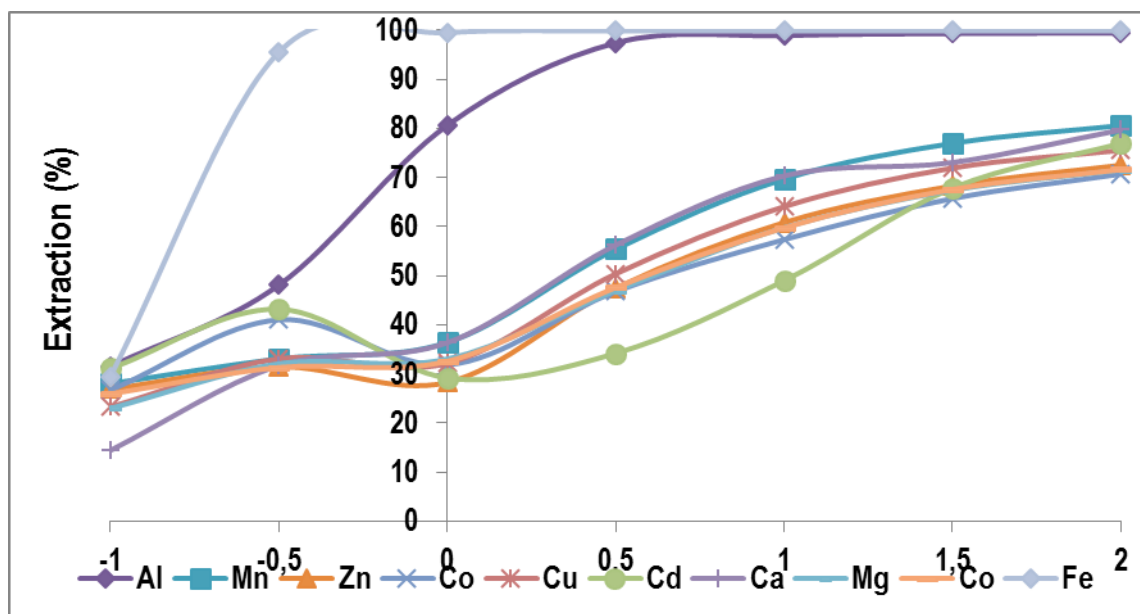


Figure 27 Extraction of transition metal in acid mine drainage with S957 with HCl

For TP207 resin while using  $\text{H}_2\text{SO}_4$ , the extraction of REE is relatively constant; although in  $-\log[\text{H}^+]$  2 and 1.5 the extraction is slightly higher; while for the rest of TM is remain between 45% and 40%.

However the extraction of TM seems to be a little more element dependent, some metals such as Fe and Cu have an extraction of 100% with higher  $-\log[\text{H}^+]$ , while the majority of them only have over 50% of extraction. While the aluminum start with 29% of extraction.

Other extraction behavior to stress would be the fact most of the TM extraction ratio do not seem to vary, with the exception of Fe and Cu and Al, as they began to drop the extraction with  $\log[\text{H}^+]$  0.5 and subsequently, when the  $-\log[\text{H}^+]$  is -1 the extraction is over 40%.



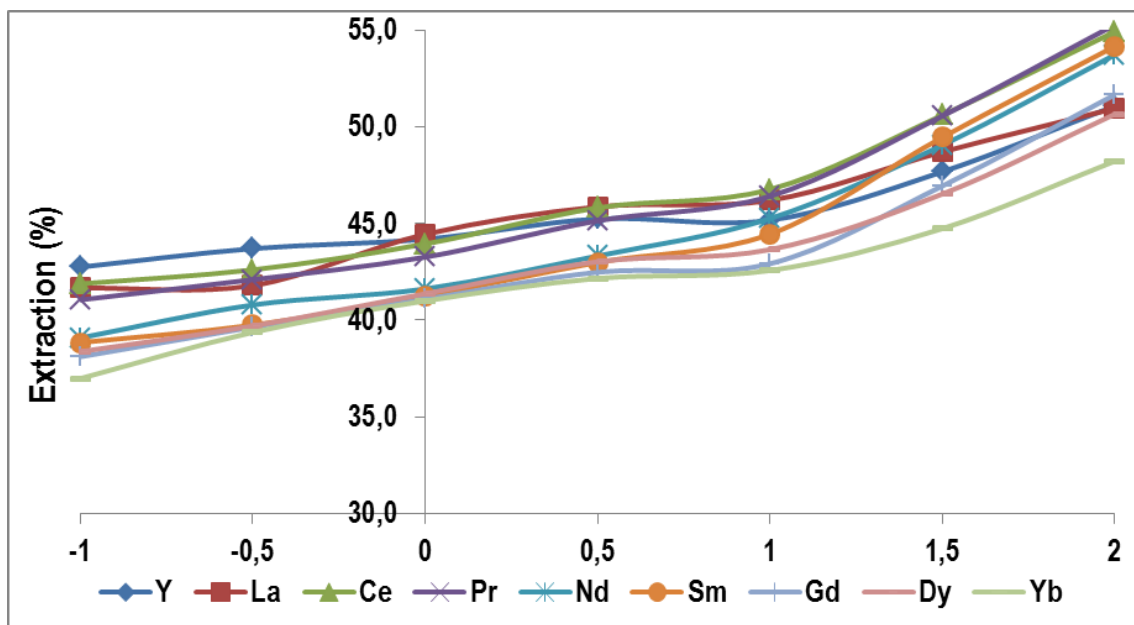


Figure 28 Extraction of REE in synthetic water with HCl with TP207

On the extraction of REE in AMD from Odiel basin abandoned mines the extraction ratio seems to be lower than synthetic water, as the extraction ratio of REE is compressed between 35% and 25%, and through the variation of  $-\log [H^+]$ , little variation of extraction can be patterned with the exception of the ph-1, where the extraction is compressed between 26% and 17%.

The extraction of TM is separated in two part, the Cu and Fe has a full extraction of 100% with  $-\log [H^+]$  between 0, and 2, and start to drop with  $-\log [H^+]$  0 and with  $-\log [H^+]$  minus than 0,5 they remain stable again, with a extraction of 30%. On other hand the rest of the TMs remain unaffected by the variation of  $-\log [H^+]$ , as they their extraction is compressed between 25% and 30% in entire curve.

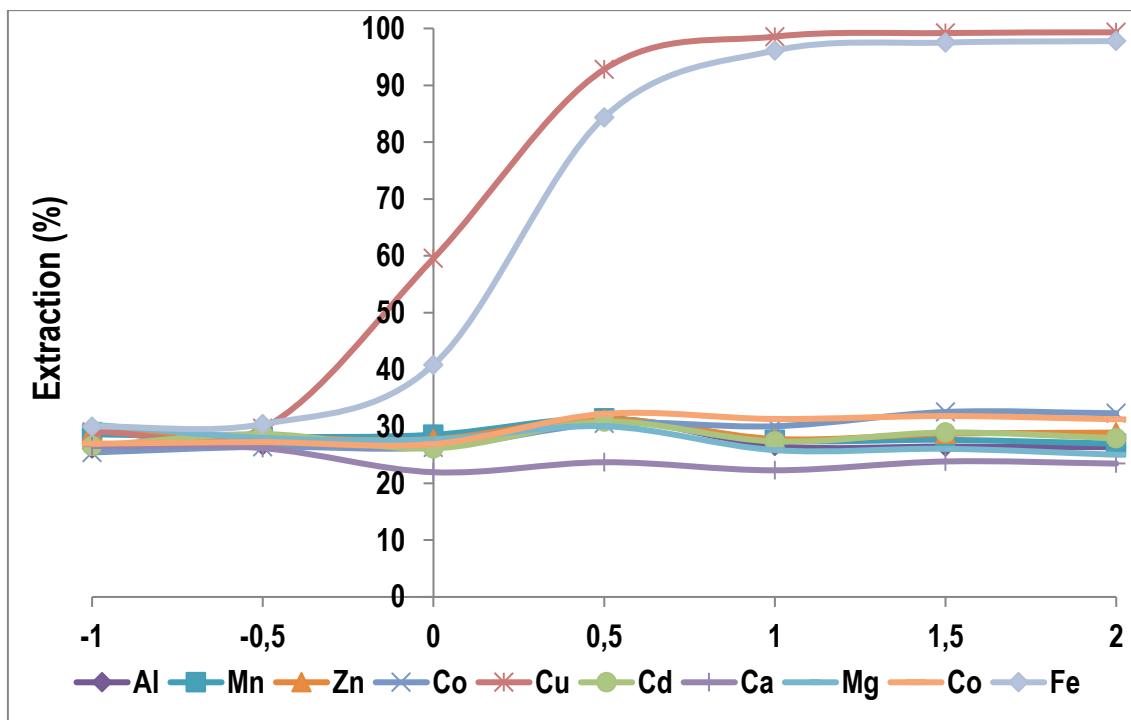


Figure 29 Extraction of transition metal in real water with TP207 with  $H_2SO_4$

If the acid used was HCl in place of  $H_2SO_4$ , the extraction ratio between different REE behaved almost invariant, the maximum at  $-\log [H^+]$  2 ranged between 47% (Pr and Ce) and 41% Yb. The extraction dropped slightly with  $-\log [H^+]$  -1 and it ranged between 42% and 38%.

The extraction of TM in this condition is also element dependent, since the variation ranged substantially, on one hand it is possible to found Mn and Co whose extraction remain unchanged during the  $-\log [H^+]$  variation, on the other hand we have Zn and Cd, whose extraction is similar to Mn and Co while on high  $-\log [H^+]$ , but have sudden rise when  $-\log [H^+]$  drops. Only Cu, which start with a 100% of extraction decreased with acidity at  $-\log [H^+] < 0,5$ .

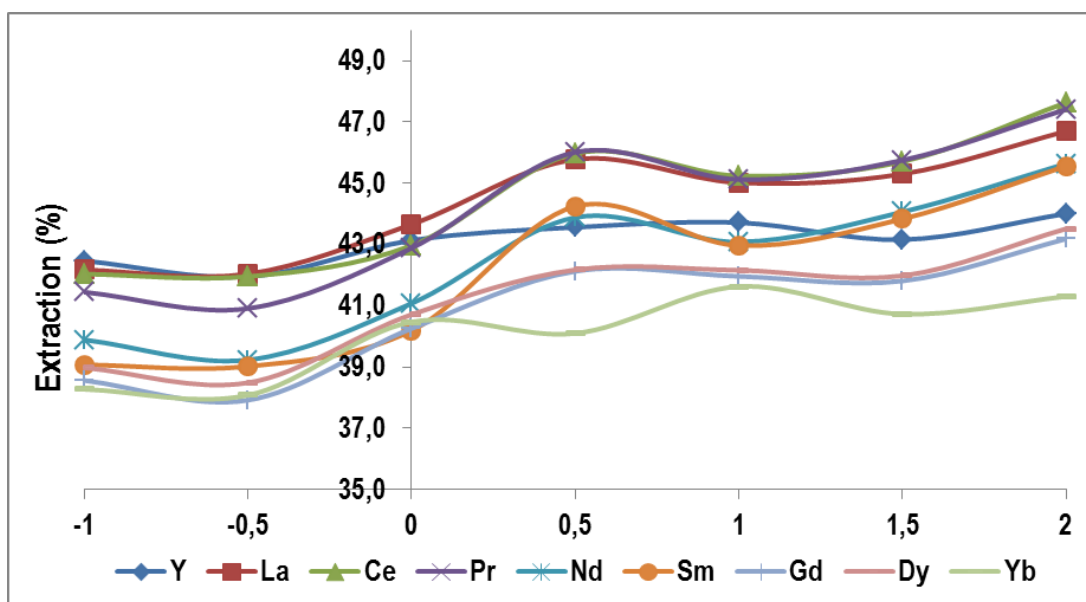


Figure 30 Extraction of REE with TP207 with HCl in synthetic water

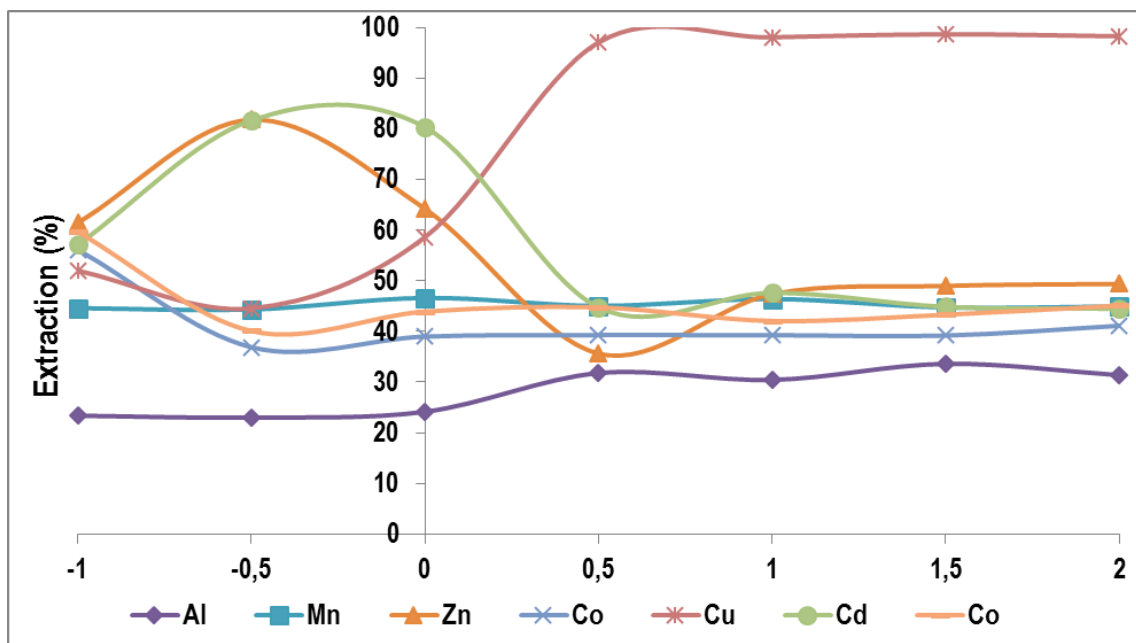


Figure 31 Extraction of transition metal with TP207 with HCl in synthetic water

Changing to extraction from AMD using HCl, REE extraction start with a range of 80%-56% at  $-\log [H^+]$  2, then drop to 31%-27% at  $-\log [H^+]$  1.5 then remain constant until  $-\log [H^+]$  0 with a sudden rise to 40% to drop again.

In case of TM extraction, Fe and Cu start with 100% extraction until  $-\log [H^+]$  0.5 then to drop to 30% of extraction in  $-\log [H^+]$  -1. Then rest of transition show a relatively stable extraction ratio, with the initial extraction being situated between 75% Co and 28% Mg. the extraction rise on  $-\log [H^+]$  0 then go back again.

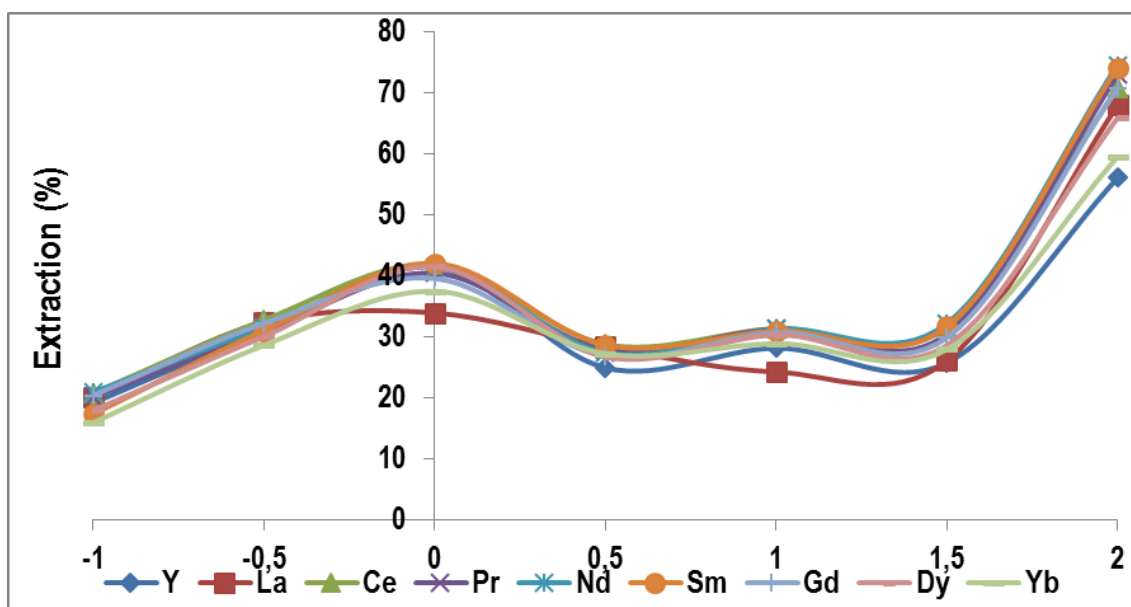


Figure 32 Extraction of REE in acid mine drainage with TP207 with HCl

### 3.6. Identification of metal extraction reactions for TP207 and S957 resins

Extraction data for both resins were analyzed to identify the nature of the metal extractions reactions involved. As numerical approach the data treatment procedures used for solvent extraction and solvent impregnated resins have been used ([Aguilar, 1987, Cortina, 1994](#)). Then, extraction data were converted to metal distribution ratios (DM) (eq 1) for both REE and TM. The metal distribution ratio is calculated from the measured metal equilibrium values and the metal resin concentration by using the low mass action as it is described by eq 1 and 17.

As the interest is centered on the identification of the metal extraction reactions involved, the metal distribution ratio could be correlated with the metal extraction reactions. Then, and taking as a reference the performance of acidic extractants in solvent extraction a relationship between both parameters could be achieved ([Peppard et al., 1958; Cortina, 1994](#))



Where concentrations of dissolved species in the aqueous phase are expressed on mol.L, and concentration of species in the resin phase are expressed as mol.Kg of resin.

Due to the complexity of the systems in terms of high ionic strength of the solutions, especially for the highest acidity conditions ( $-\log [H^+] < 1$ ), and for the complexation of dissolved species, e.g. TM and REE in solution, a preliminary data treatment was performed. Additionally, the total functional group concentration on the resin phase was fixed as the total resin capacity. Although in the case of S957, two types of functional groups are present, the content of aminophosphinic content was only considered.

The metal extraction equilibrium constant  $KML_3$  is defined by eq 15:

$$K ML_3 = \frac{\overline{ML_3}[H]^3}{[M^{3+}][HL]^2} \quad \text{Equation (16)}$$

Taking into account that  $K = D * \frac{[H^+]^3}{[HL]^3}$ , log K could be calculated by Eq 18

$$\log(K) = \log(D) + 3 * \log[H^+] - 3\log(HL)r \quad \text{Equation (17)}$$

$$\log(D) = \log(K) - 3 * \log[H^+] + 3\log(HL)r \quad \text{Equation (18)}$$

Then a graphical treatment of the extraction data was carried and the %Ex percentage values were converted to  $\log D_M$  and they were represented as a function of the  $-\log [H^+]$  for a given functional resin concentration (g/L).

Analysis of the speciation data, using the Hydra data base and the Equilibrium Calculation Code Medusa (Puigdomenech, 2010) for a model TM and REE solution assuming a total concentration of 2M sulphate is shown in Figure 33. As it can be seen the complexation for REE elements from the  $M^{3+}$  to  $MSO_4^+$  and  $M(SO_4)_2^-$  is favored with the decrease of the acidity ( $-\log[H^+]/pH$ ).

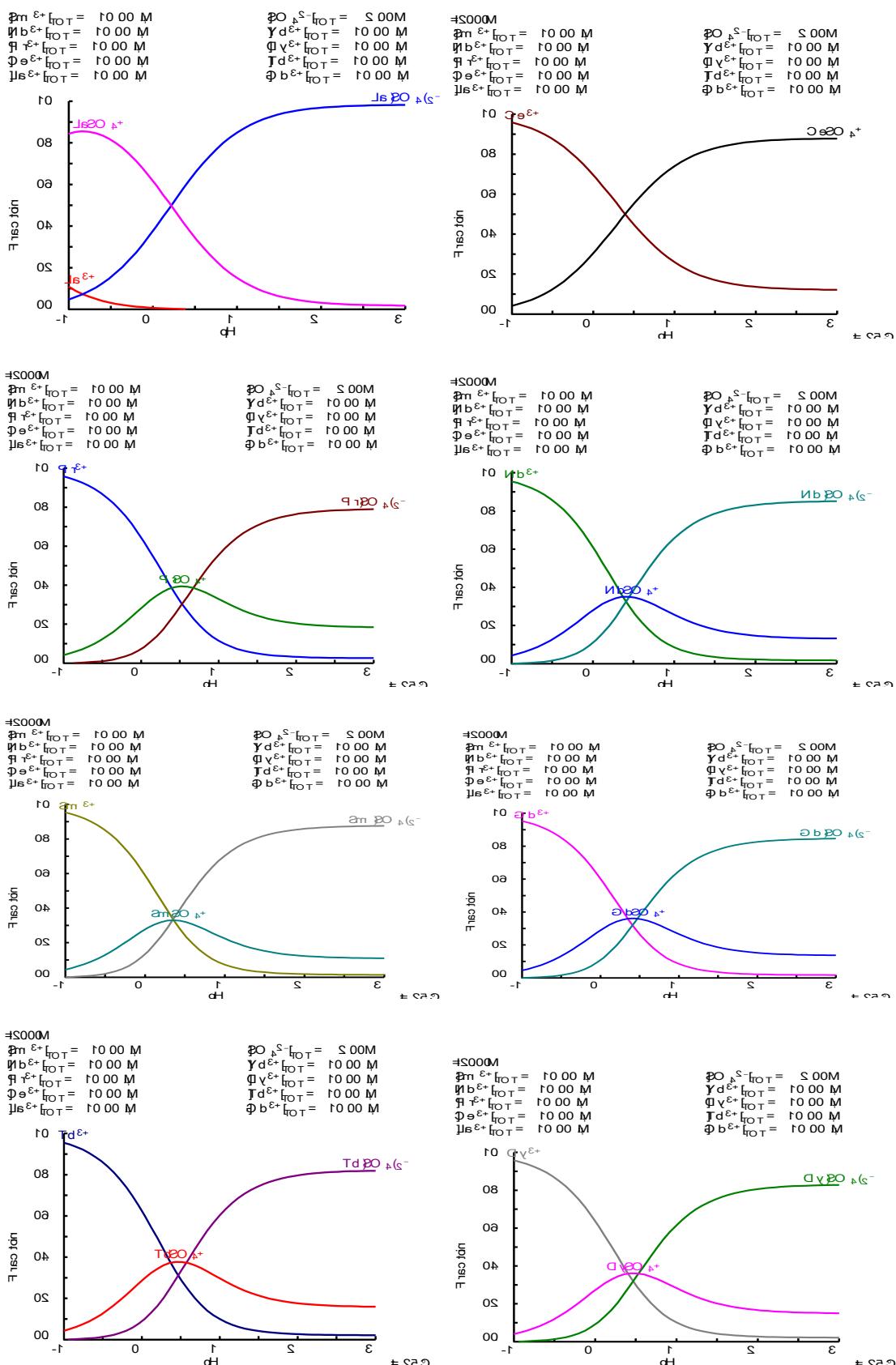


Figure 33 Figure variation of the relative abundance of  $Ca(II)$ ,  $Co(II)$ ,  $Cu(II)$ ,  $Zn(II)$ ,  $Mg(II)$ ,  $Mn(II)$  aqueous species with pH in in sulphuric solutions  $[SO_4] = 5 \text{ M}]$ . Thermodynamic data from MEDUSA database (Puig-Domenech, 2010).

Values of log D as a function of  $-\log [H^+]$  for S957 and TP207 resins are plotted in figure 34, 35, 36 and 37. For the case of REE the dependence is linear and the linear regression analysis of the  $\log D/\log[H^+]$  functions is summarized in table 19. Values obtained ranged from 2.6 to 3, indicating that the extraction process is taking place according to the formation of 1/3 complexes (Metal/functional group) as describes reaction. For the cases of linear dependence, the origin ordinate (intercept) from the linear regression analysis de KML3 constant could be calculated if the free functional concentration is calculated.

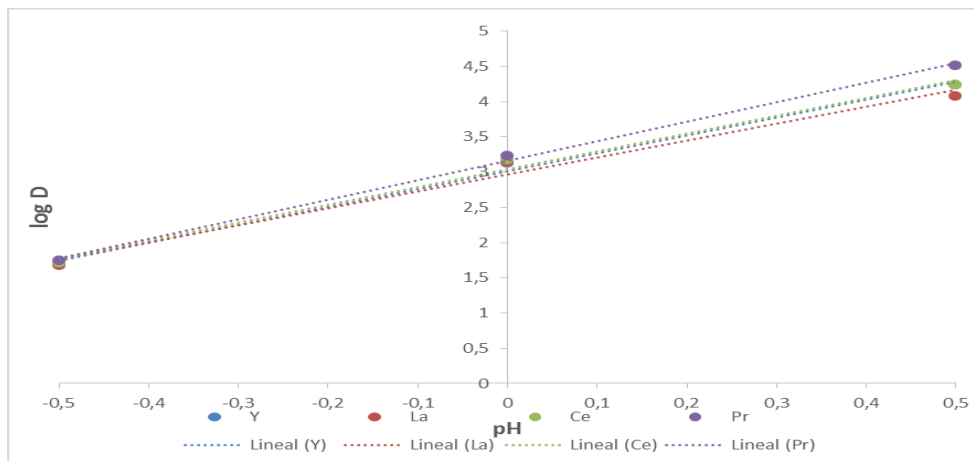


Figure 34 logarithmic graph of distribution ratio of Y, La, Ce and Pr

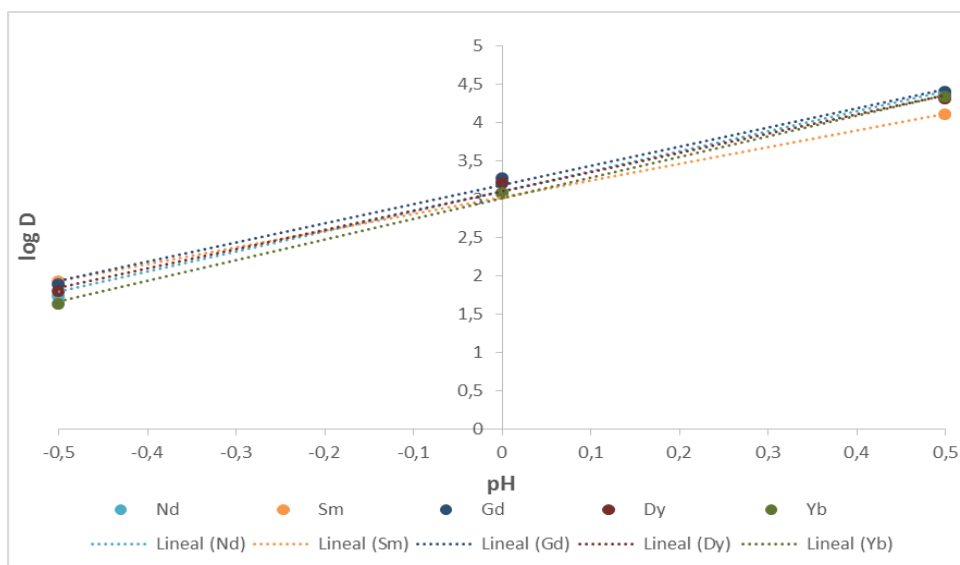


Figure 35 logarithmic graph of distribution ratio of Nd, Sm, Gd, Dy and Yb

Table 19 slope of logarithmic graph of transition metals and REE

Transition metal	slope	intercept	REE	slope	Intercept
Al (III)	1,9	2,2	Y	2,5	3
Mn (II)	1,4	1,5	La	2,4	3
Cu(II)	1,7	1,2	Ce	2,5	3
Zn(II)	1,1	1,3	Pr	2,8	3,2
Co(II)	1,1	1,2	Nd	2,6	3
Cd(II)	1,4	1,5	Sm	2,2	3
Ca(II)	0,6	0,5	Gd	2,5	3,2
Mg(II)	0,6	0,8	Dy	2,5	3,2
Fe (III)	2,7	3,6	Yb	2,7	3

Analysis of the logDM values as a function of log [H<sup>+</sup>] for transition metals with oxidation state +II show also a wide variation, with values from 1.7 up to 0.6. For metals in the oxidation state (+3) as Fe(III) and Al (III) shown an slope +3, for Fe(III) and +2 for Al(III). This behavior is associated to the complexation behavior of both elements in sulfuric solutions. As it is shown in figure 36, a higher complexation of Al(III) with SO<sub>4</sub><sup>2-</sup> and then the extracted complexes could be ionic forms in double and single charged species.

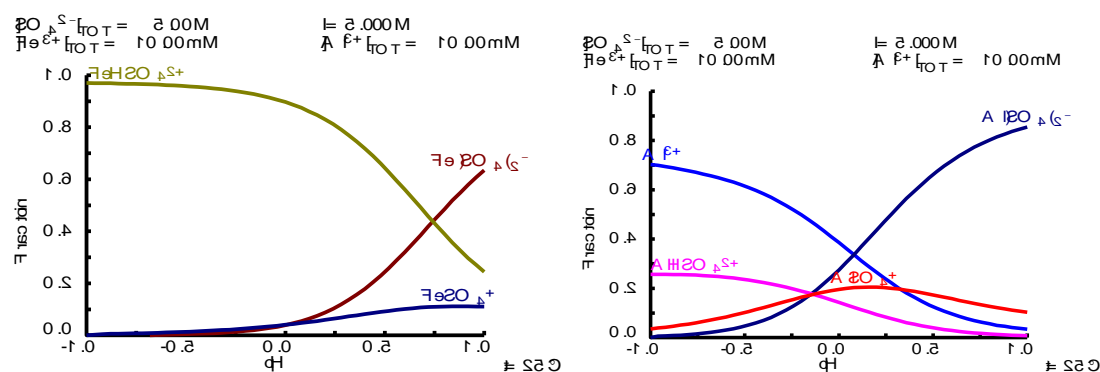


Figure 36 variation of the relative abundance of Ca(II), Co(II), Cu(II), Zn(II), Mg(II), Mn(II) aqueous species with pH in in sulphuric solutions [SO<sub>4</sub>]= 5 M]. Thermodynamic data from MEDUSA database (Puig-Domenech, 2010).

The variation of logDM values for TM as a function of the acidity it is swon in in Figure 37 and Figure 38.

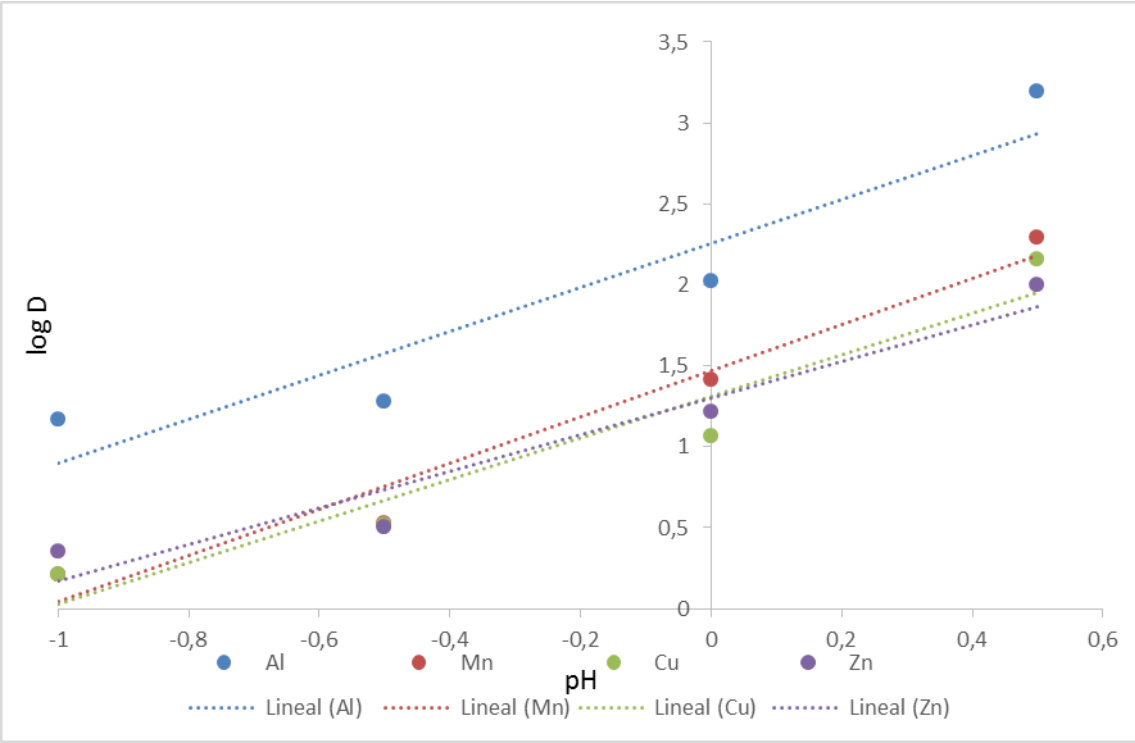


Figure 37 Variation of log D values of TM ( Al, Mn, Cu and Zn) as a function of thr acidity

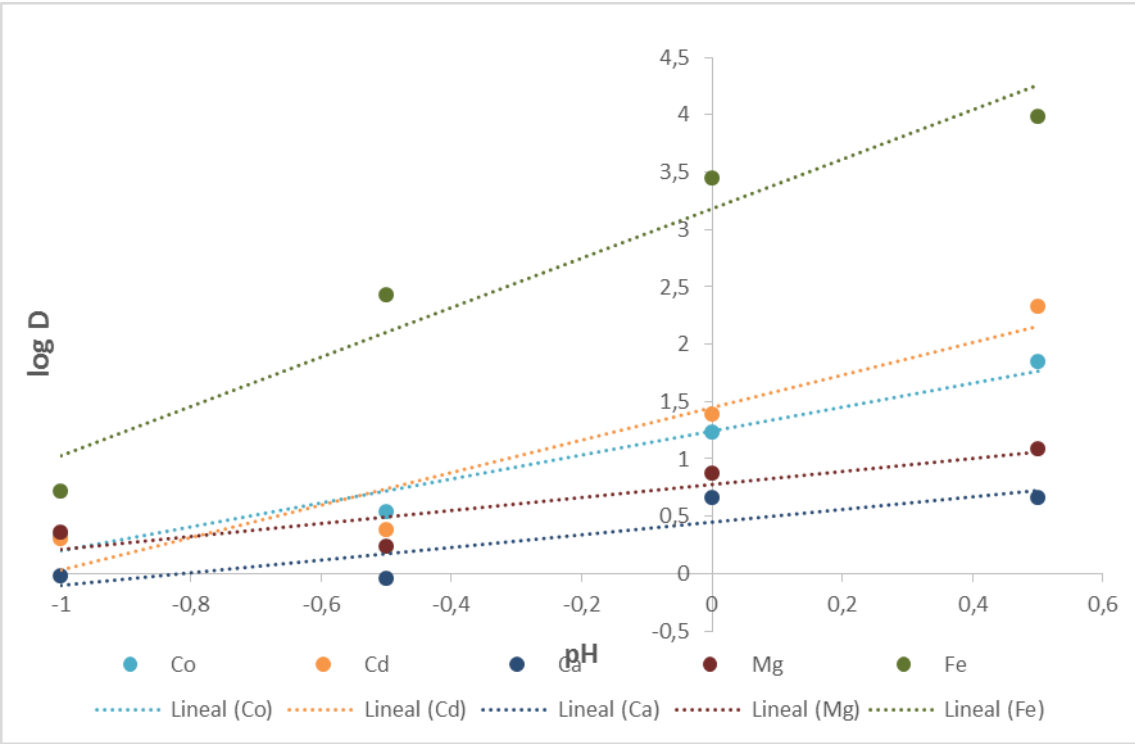


Figure 38 Variation of log D values of TM (Co, Cd, Ca, Mg and Fe) as a function of thr acidity of



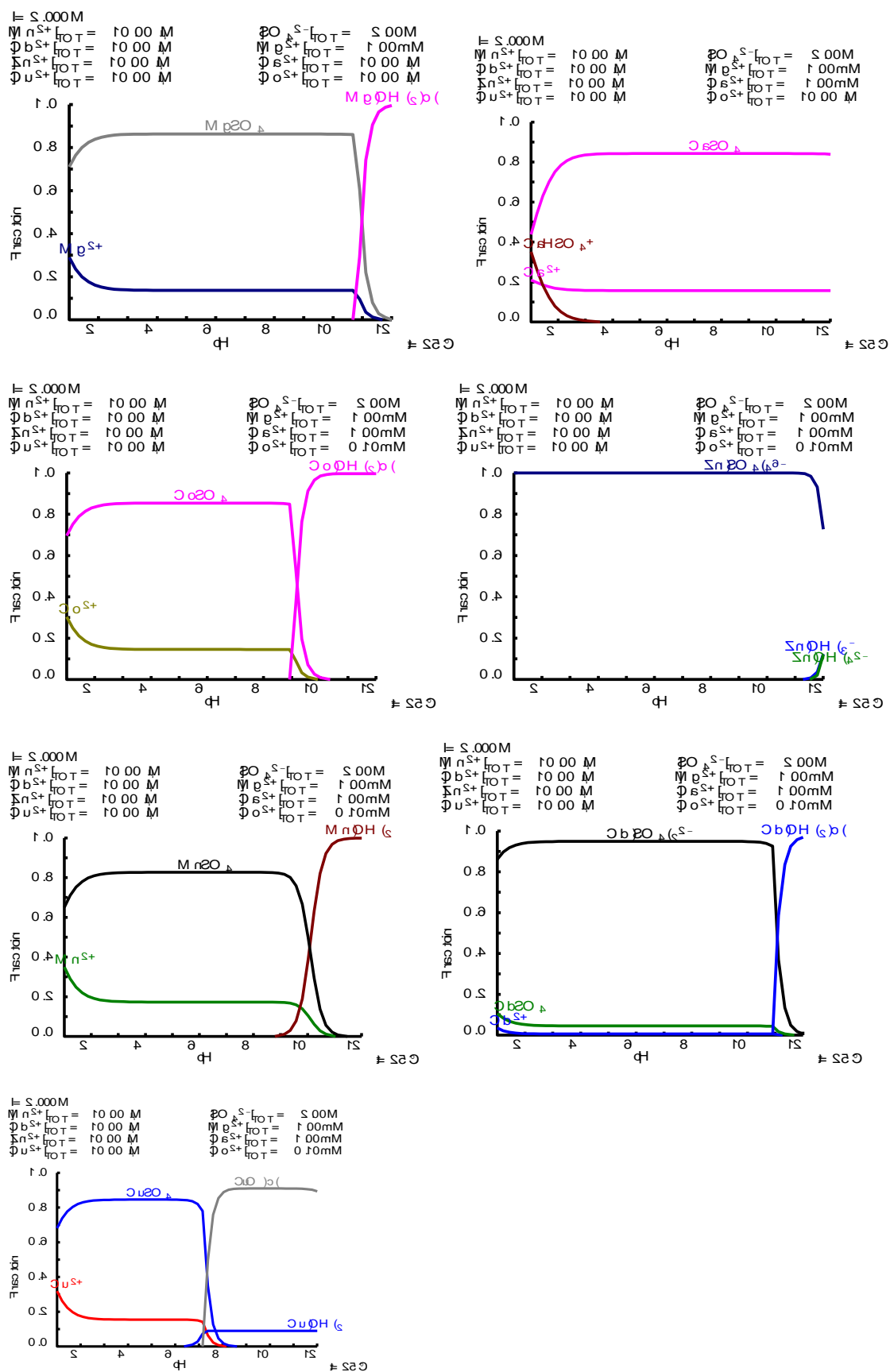


Figure 39 Variation of the relative abundance of Ca(II), Co(II), Cu(II), Zn(II), Mg(II), Mn(II) aqueous species with pH in sulphuric solutions  $[\text{SO}_4] = 5 \text{ M}]$ . Thermodynamic data from MEDUSA database (Puig-Domenech, 2010).

As it is seen in the previous figures (24-32), there is always a point in the  $-\log[H^+]$  variation where transition metal ions extraction began to drop while REE extraction still remains strong. For resin TP 207, this point would be around  $-\log[H^+]$  around 1 and for resin S957 this point would be  $-\log[H^+]$  0.

### 3.7. Resin saturation assays using extraction cycles

A sorption cycle (of three stages) was carried to reach the resin saturation, working at conditions of acidity where the maximum extraction capacity could be achieved (e.g.  $-\log[H^+] < 1$ ). For S957 resin, REE extraction results was just as expected, in the first round, the resin extracted over 60% of the REE present in ADM, in the second round the same resin extracted 20% of the REE present in the solution, however in the third step the resin have reached its saturation in REEs. The profiles of the saturation experiment are shown in figures 40 and 41. From values of extraction the sorption capacity for REE was calculated and values are summarized in table 20.

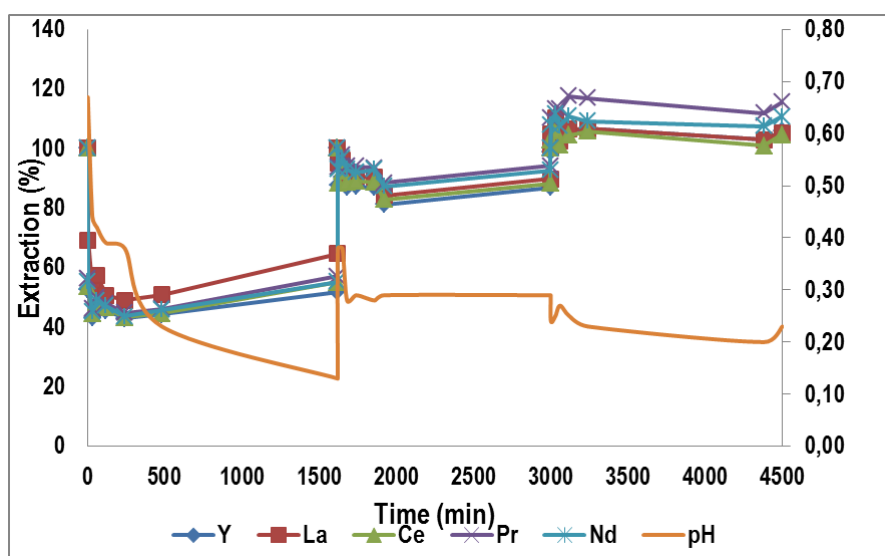


Figure 40 Y, La, Ce, Pr and Nd extraction saturation profiles with S957 and pH variation along three loading cycles.

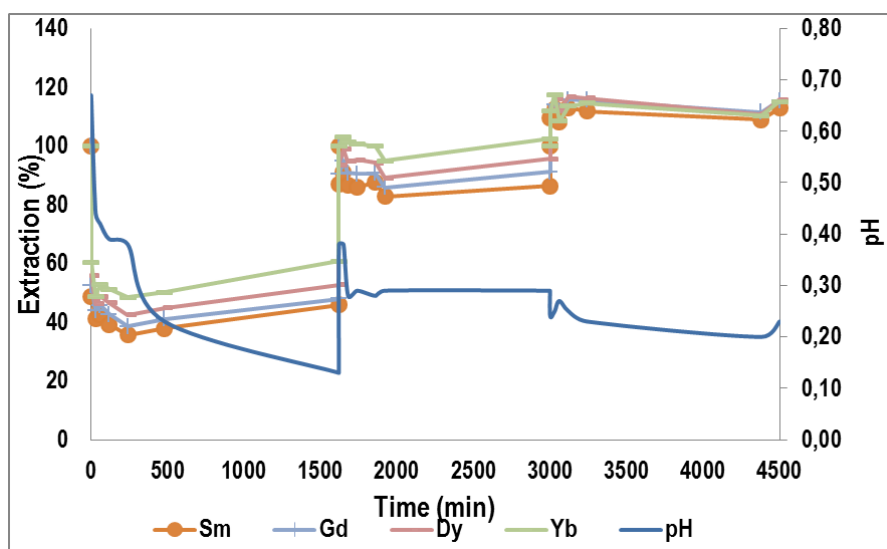


Figure 41 Sm, Gd, Dy and Yb extraction saturation profiles with S957 and pH variation along three loading cycles.

Table 20 . Collection of REE capacity from cycling experiments with S957 resin

(meq/g)	Y	La	Ce	Pr	Nd	Sm	Gd	Dy	Yb
Round 1	1,74E-04	3,55E-05	1,48E-04	1,59E-05	7,57E-05	2,51E-05	2,95E-05	2,03E-05	6,28E-05
Round 2	4,74E-05	1,03E-05	3,87E-05	2,15E-06	1,26E-05	6,34E-06	5,06E-06	1,93E-06	3,87E-06
Round 3	2,09E-05	5,41E-06	1,53E-05	5,75E-06	1,82E-05	5,95E-06	8,76E-06	6,80E-06	2,42E-05
total	2,42E-04	5,12E-05	2,02E-04	2,38E-05	1,07E-04	3,74E-05	4,33E-05	2,90E-05	9,09E-05
Sum									8,26E-04

For the case of TM, the extraction in the first step is over 15%, the second is over 10% and third also 10%. Those low extraction ratios are explained by the higher concentrations of those elements. The extraction ratios, do vary depending on the metal nature. Metals such as Al and Cd are more extracted in the third step while others like Co and Mg have an extraction over 10%. However Fe is almost full extraction all three rounds.

In Table 20 and 21 the total capacity of resin used in REE and transition metal, being  $8,26 \times 10^{-4}$  and 1,99 meq/g respectively. As reason of such difference would the concentration of each of them present in the sample, on the low  $-\log [H^+]$ , even though the extraction ratio of transition metal is rather low, the overall extraction of transition metal is still higher than REE. Also is interesting to notice that Iron and Al has a rather high extraction ratio even in low  $-\log [H^+]$ .

Another interesting fact to notice is that the resin has already passed its saturation point (Table 14), since the resin maximum capacity is 1,3 meq/g (according to resin total capacity) and the resin experiment reached 1,9. As most of the metals are complexed, most of the cations are present as monocharged species and the exchange capacity of the resin should be higher, assuming that cations are present on its oxidation state form (e.g.  $M^{2+}$  or  $M^{+3}$ ).

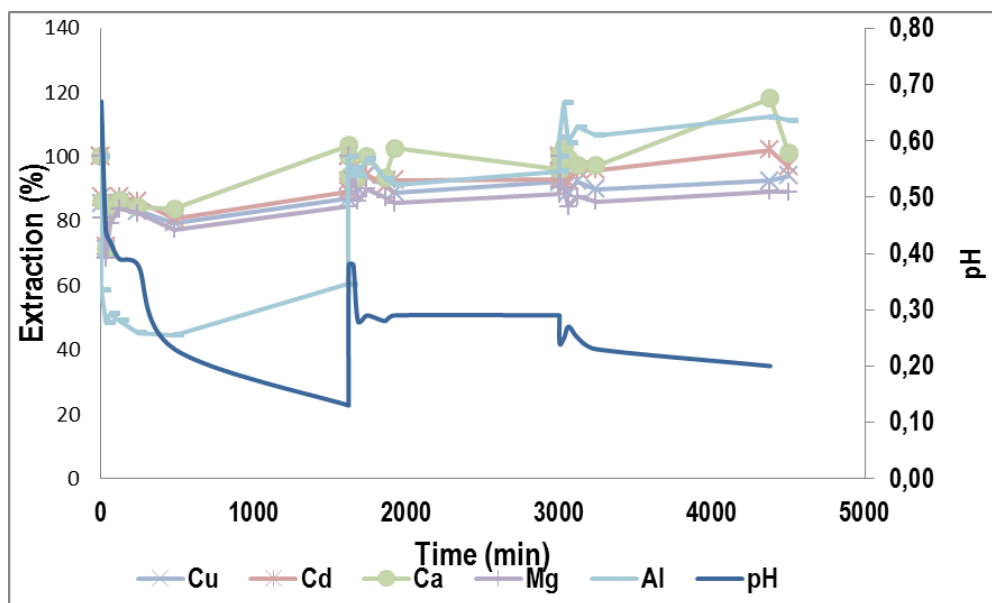


Figure 42 Cu, Cd, Ca, Mg and Al extraction saturation with S957 and pH variation along three loading cycl

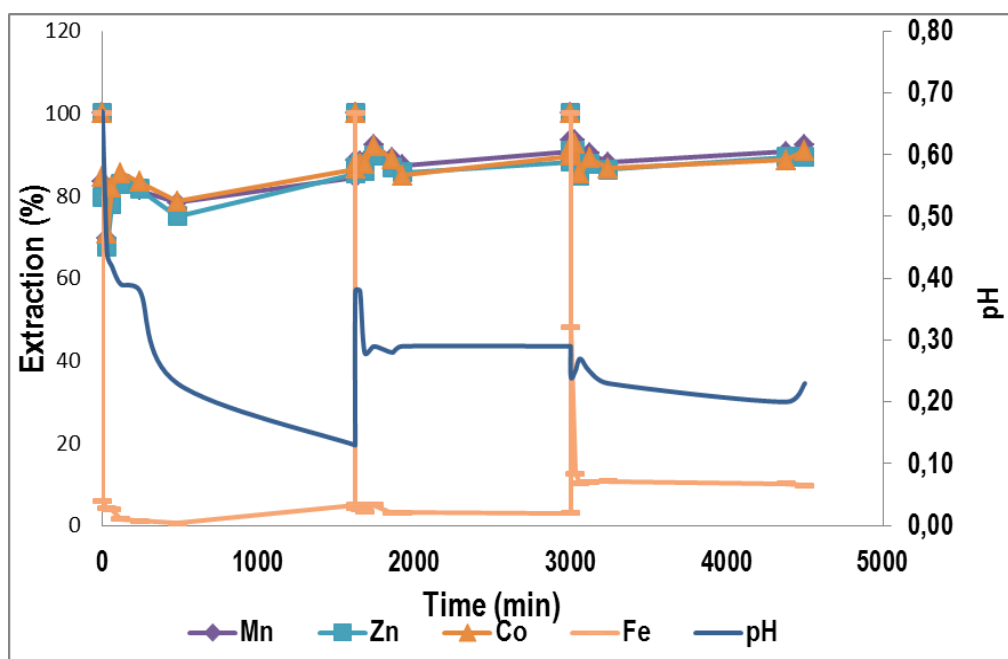


Figure 43 MN, Zn, Co and Fe extraction saturation with S957 and pH variation along three loading cycle

Table 21. Collection of transition metal capacity from cycling experiments with S957 resin

(meq/g)	Mn	Zn	Co	Cu	Cd	Ca	Mg	Al	Fe
Round 1	1,02E-02	1,11E-02	2,74E-04	4,67E-03	1,90E-05	6,65E-03	1,80E-01	4,95E-01	2,66E-01
Round 2	6,11E-03	8,88E-03	2,10E-04	2,78E-03	1,21E-05	7,29E-03	1,35E-01	5,67E-02	2,72E-01
Round 3	5,05E-03	8,00E-03	1,83E-04	2,08E-03	5,56E-06	2,36E-03	1,27E-01	1,44E-01	2,53E-01
Total	2,14E-02	2,80E-02	6,67E-04	9,53E-03	3,67E-05	3,00E-03	4,42E-01	6,96E-01	7,92E-01
Sum									1,99E+00

For the resin TP 207, the extraction capacity for both REE and TM were much lower and after the first sorption cycle the resin was saturated. The variation of metal concentration are shown in Figures 44 to Figure 47 and the sorption capacities collected in Table 22 and Table 23, extraction in REE stop with the first round, the other round doesn't have any extraction at all.

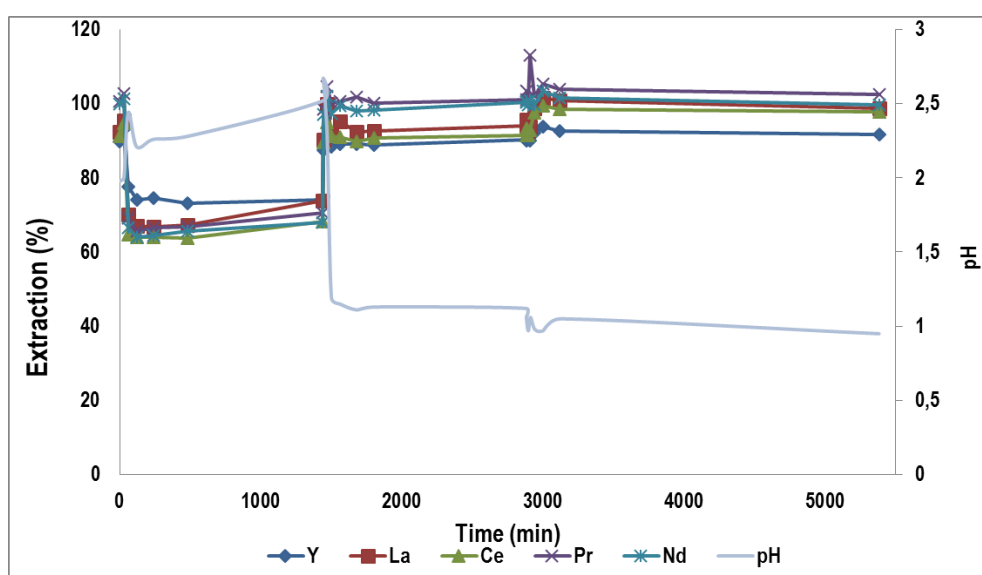


Figure 44 Y, La, Ce, and PR extraction saturation with TP207 and pH variation along three loading cycle

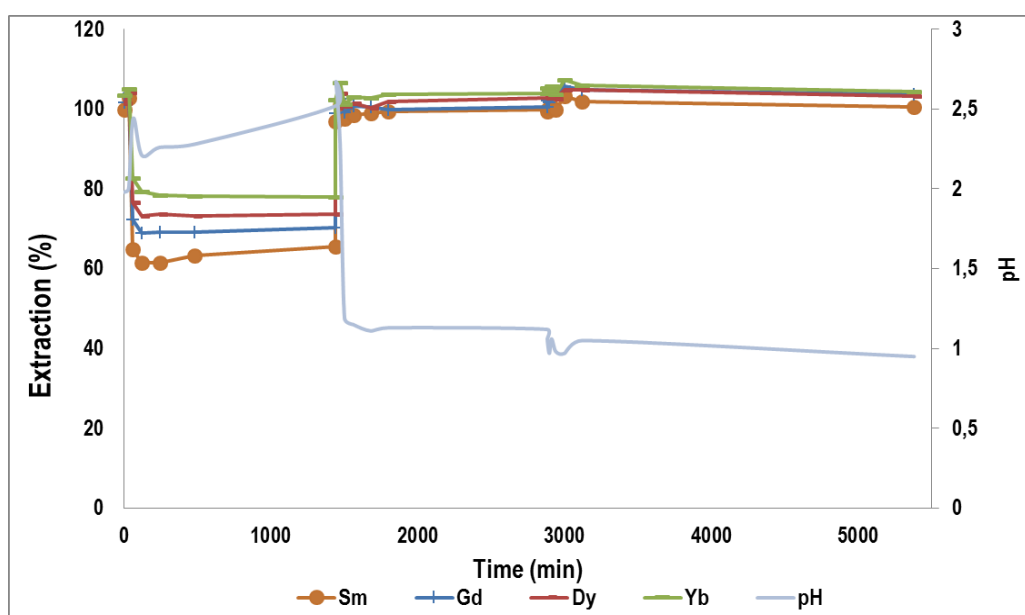


Figure 45 Sm, God, DY and by extraction saturation with TP207 and pH variation along three loading cycle

Table 22 . Collection of REE capacity from cycling experiments with TP 207resin

(meq/g)	Y	La	Ce	Pr	Nd	Sm	Gd	Dy	Yb
Round 1	9,40E-05	2,63E-05	1,05E-04	1,10E-05	5,42E-05	1,59E-05	1,68E-05	1,14E-05	3,54E-05
Round 2	3,52E-05	5,89E-06	2,82E-05	4,20E-07	5,25E-07	8,23E-08	3,17E-07	1,19E-06	6,20E-06
Round 3	3,03E-05	1,22E-06	7,21E-06	9,53E-07	7,18E-07	2,73E-07	2,11E-06	1,40E-06	7,02E-06
Total	1,60E-04	3,34E-05	1,40E-04	1,24E-05	5,54E-05	1,63E-05	1,92E-05	1,40E-05	4,86E-05
Sum									4,99E-04

For transition metal, a very similar scenario happens, most of the transition stop in the first round or continue with insignificant extraction with exception of Fe whose extraction, alongside with Cu, is almost 100% in the first round, and 65% the second round and in the third round the extraction is over 30%.

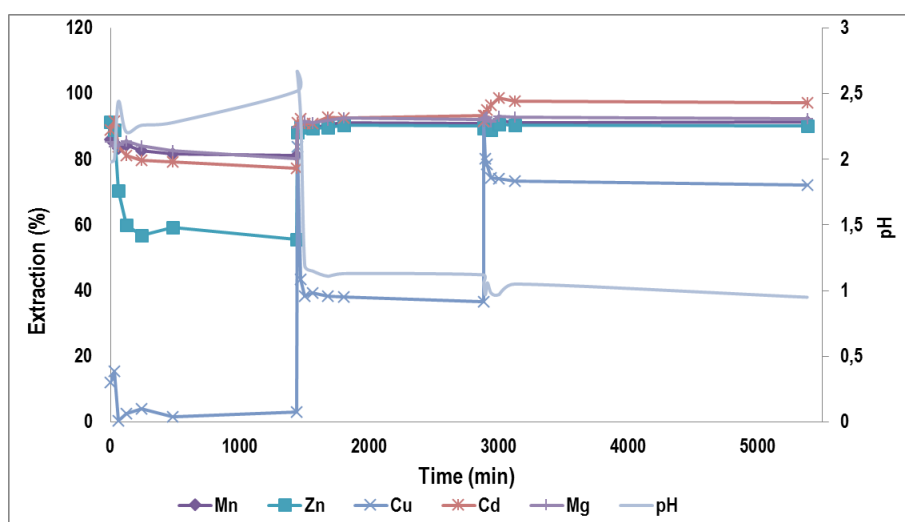


Figure 46 Mn, Zn, Cu, Cd and Mg extraction saturation with TP207 and pH variation along three loading cycle

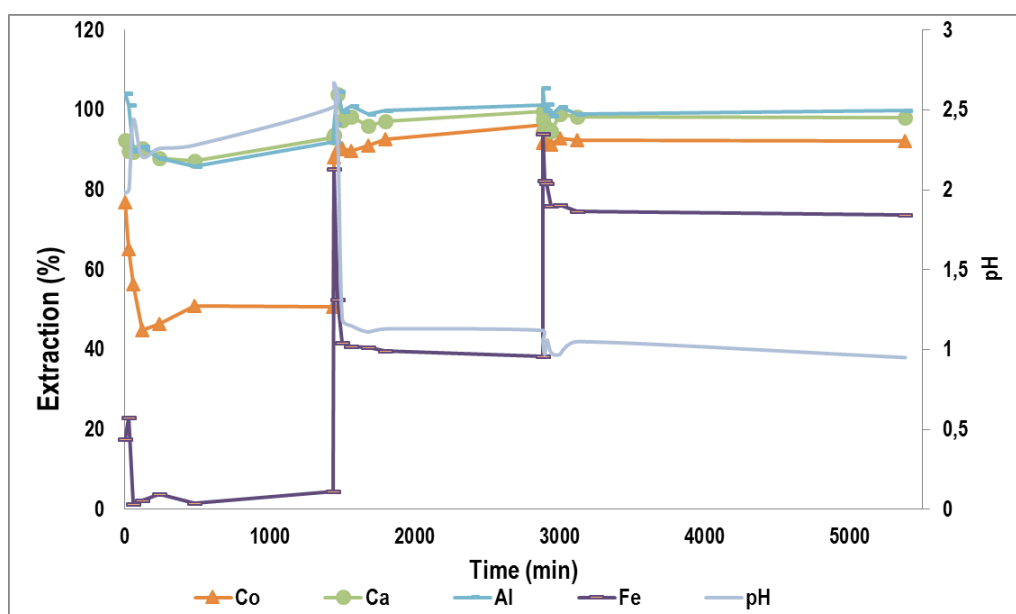


Figure 47 Co, Ca, Al and Fe extraction saturation with TP207 and pH variation along three loading cycle

Table 23 Collection of transition metal capacity of resin TP 207.

(meq/g)	Mn	Zn	Co	Cu	Cd	Ca	Mg	Al	Fe
Round 1	1,23E-02	3,37E-02	1,00E-03	3,50E-02	4,06E-05	1,24E-02	2,33E-01	9,90E-02	2,68E-01
Round 2	5,91E-03	7,39E-03	7,60E-05	2,29E-02	1,17E-05	5,09E-04	9,18E-02	1,67E-02	1,73E-01
Round 3	5,60E-03	7,43E-03	1,59E-04	1,00E-02	4,75E-06	3,30E-03	8,82E-02	1,58E-03	7,40E-02
Total	2,38E-02	4,85E-02	1,23E-03	6,78E-02	5,70E-05	1,62E-02	4,12E-01	1,17E-01	5,15E-01
Sum									1,20E+00

Similar scenario can be spotted here, the REE occupy a really small amount of capacity, and transition metals still dominate, by same reason. The one difference would be in this case the resin has yet to reach to saturation.

Is interesting to notice that in this situation the resin is still far from saturating, since the resin maximum capacity for resin TP 207 according to Table 14 is 3,07 meq/g and in in this experiment the resin only used over 1,2 meq/g. However the resin has stopped the REE absorption fairly early in the first round.

## Project planning and economical evaluation

- Project cost

Three different categories have been considered to have an estimation of the total cost of the project: Materials and Reagents, Energy consumption and Human resources.

Materials and reagents used during the experimental phase are summarized in Table 24.

Table 24 Material and reagent used during experimental phase.

	Amount (g)	Cost(euro/g)	Total cost (euro)
Al <sub>2</sub> (SO <sub>4</sub> ) <sub>3</sub>	12,4	14,4	178
ZnSO <sub>4</sub> · 7H <sub>2</sub> O	4,4	7,2	31,8
CaSO <sub>4</sub>	4,3	15,8	67,9
CuSO <sub>4</sub>	2,5	3,3	8,3
La <sub>2</sub> (SO <sub>4</sub> ) <sub>3</sub>	2,6	2,7	7
Yb <sub>2</sub> O <sub>3</sub>	0,6	4,7	2,7
Dy <sub>2</sub> O <sub>3</sub>	0,2	5,0	1,2
Pr(NO <sub>3</sub> ) <sub>3</sub> · 6H <sub>2</sub> O	0,8	1,5	1,2
SmCl <sub>3</sub>	0,4	2,6	1,1
NdCl <sub>3</sub> · H <sub>2</sub> O	0,6	1,1	0,7
MgSO <sub>4</sub>	10,1	0,2	1,7
FeSO <sub>4</sub> · 7H <sub>2</sub> O	45	0,4	2
CdSO <sub>4</sub> · 8H <sub>2</sub> O	2,3	12	27,3
MnSO <sub>4</sub> · H <sub>2</sub> O	3,0	0,3	0,8
CoSO <sub>4</sub> · 7H <sub>2</sub> O	4,5	0,7	3,2
Y <sub>2</sub> O <sub>3</sub>	1,3	7,9	10
Sum			344,7

Energy used by equipment during the experiment and analysis cost can be found in the Table 25 and 26.

*Table 25 Cost of sample's analysis*

	Amount of samples	Unit cost (euro)	Total (euro)
ICP-MS/ICP-OES	1,50E+02	21,13	3,17E+03
Atomic absorption	2,40E+01	20	4,80E+02
Sum			3,65E+03

*Table 26 Energy consumption*

	Consumption (kWh)	Unit cost (euro/kWh)	Total (euro)
Agitator	15,0	0,15	2,25
Refrigerator	7,9		1,19
Oven	130		19,5
Vacuum	5		0,75
Sum			23,7

Human resources cost is summarized in Table 27

*Table 27 Cost of human resources*

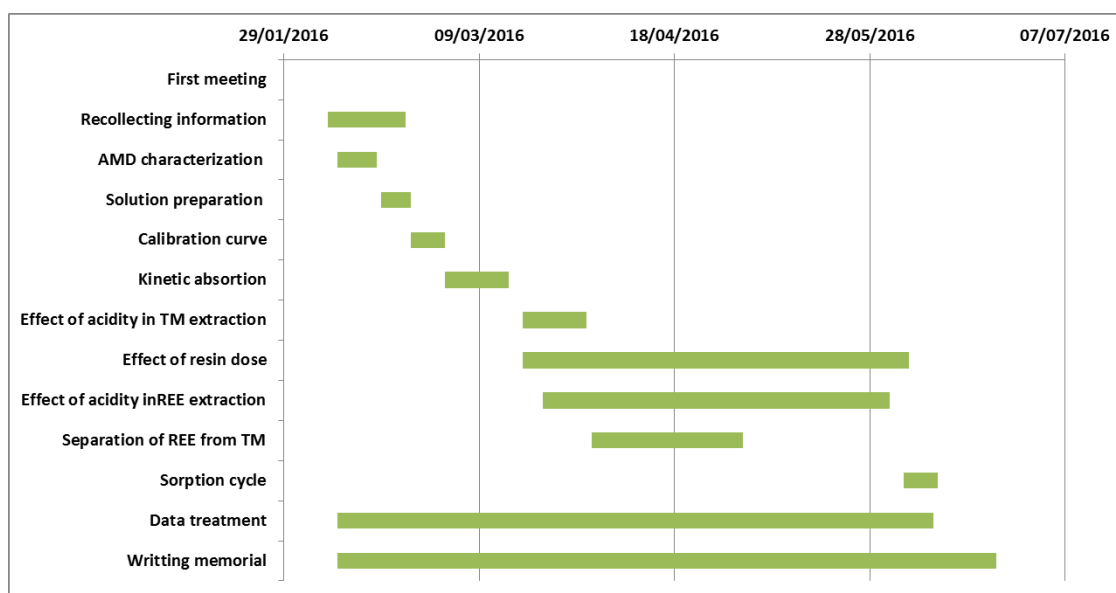
	amount	Salary (euro/h)	time(h)	total cost
engineer	1	15	600	9000
supervisor	2	40	40	3200
Sum				12200

The total cost for this project would be 16218,4 euro, however this is only a estimation of the real cost, the real cost may be higher.

The overall planning of the entire project is summarized in the following diagram Table 28.



Table 28 The Project planning



## Environmental assessment/sustainability issues

The wastes generated during the experimental phase were disposed accordingly; the solutions with pH below 4 were disposed in the container for residual pH solution. The solution containing REE were saved separately for later uses, the solution containing arsenazo III were disposed in the container for organic solution.

The project is purely experimental in laboratory scale, no further study of environmental impact was deemed to be necessary.

In case of larger scale, then the disposal of REE stripped AMD should be consider, as the solution can have serious environmental impact because of it acidity.

## Conclusions

To come to the point, we can conclude that:

- a) Analysis of secondary resources containing REE
  - Both solid and AMD contain REE worth of recovery, the leachate of solid contains more significant amount of REE in comparison with AMD, and the concentration increase with the depth.
  - Samples leached with HCl have more REE than samples obtained by leaching with H<sub>2</sub>SO<sub>4</sub>.
  - The most notable REE in the AMD are La, Ce, Nd and Y while the leachate have a similar distribution, although the concentration from samples with caustic magnesia seem to be dime in comparison.
- b) Evaluation of the extraction of REE with two ion exchange resins
  - The extraction and its separation is indeed possible with resin TP 207 and S957 by lowering the pH of the AMD. S957 show more potential in extracting REE and separating them from transition metal in comparison with TP 207, however the latter seem to be potentially easier to strip than S957, since for S957 a much lower pH would be required for this to happen. The  $-\log [H^+]$  necessary for the separation of REE from transition metal with S957 would be 0 and for TP 207 1. For both resin traces of transition metal still can be seen in the extraction, for this reason a more aciditic condition need to be tested.
  - The resin TP 207 have a higher capacity in comparison with S957, however it does not show selectivity with REE, as it stop extracting REE in fairly early stage while keep extracting TM. On other hand, the resin S957, while has lower capacity, it keep extracting REE from the solution until it capacity is full.
- c) Identification of metal extraction reaction.
  - The experimental data confirmed that the main reaction involved on the extraction of REE follow the general equation:
  - $$M^{3+} + 3\overline{HLr} = \overline{ML_{3,r}} + 3H^+$$
  - While for the case of TM the metal speciation is affecting the extraction reactions and the number of involved ligands number of functional (groups HL) n are typically below the oxidation state number

## Acknowledgments

This study has been supported by the Waste2Product project (CTM2014-57302-R) financed by Ministry of Science and Innovation and the Catalan government (project ref. 2014SGR050). The authors gratefully acknowledge Dr. C. Ayora and Dr. E. Torres (CSIC-IDAEA) for AMD waters and REE containing solid waste samples. Lanxess Iberica and Puolite Iberica for resins samples supply.

The author would also like to thanks Prof José Luis Cortina and Doctor Mehrez Hermassi for their guidance in this project and also Blai Pineda for his help in laboratory.

## Reference

- Adam Jordens, Ying Ping Cheng, Kristian E. Waters. 2013. A review of the beneficiation of rare earth element bearing minerals. *Minerals Engineering*. 97-114.
- Aguilar. M, *Developments in Solvent Extraction*, R.A. Chalmers and M. Mason, Ellis Horwood, Chichester, 1988, p 87.(1988)
- Alguacil F.J., F. Rodríguez. 1997. Procesos de separación de las tierras raras. *Rev. Metal Madrid*.
- Anton R. Chakhmouradian, Frances Wall. 2012. Rare Earth Elements: Minerals, Mines, Magnets (and More). *Mineralogical Magazine*.155-163.
- Astrom M.E., Osterholm P., Gustafson J.P. Nystrand M., Peltola P., Nordmyr L.andBoman A. (2012) Attenuation of rare earth elements in a boreal estuary. *Geochimica et Cosmochimica Acta* 96: 105–119
- Bradbury M.H. and Baeyens B. (2002) Sorption of Eu on Na- and Ca-montmorillonites: Experimental investigations and modelling with cation exchange and surface complexation. *GeochimicaetCosmochimicaActa*, 66: 2325-2334
- Brown, D., Ma, B.M., Chen, Z., 2002. Developments in the processing and properties of NdFeb-type permanent magnets. *Journal of Magnetism and Magnetic Materials* 248, 432–440.
- Carlos Ayora, Francisco Macías, Ester Torres, José-Miguel Nieto. 2013. Rare earth elements in acid mine drainage.
- Castro Pay. 2015. Eliminació d'ions trivalents d'aigües salobres mitjançant nanofiltració: Efecte de la concentració de la sal dominant.
- Chul Woo Nama, Pankaj Ku. Parhia, Kyung Ho Park, Smruti Pr. Barika, Jean Tae Parka.2013. Recovery of Total Rare Earth Metal from Deep Sea Nodule Leach Liquor by Solvent Extraction Process. *The International Society of Offshore and Polar Engineers (ISOPE)*. p157.
- Coppin F., Berger G., Bauer A., Castet S. and Loubet M. (2002) Sorption of lanthanides on smectite and kaolinite. *Chemical Geology*, 182: 57-68
- Cortina J.L, N.Miralles, M.Aguilar, A.M. Sastre. 1994. *Hydrometallurgy* 36 (2) 131-142.
- Delgado J., Pérez-López R., Galván L., Nieto J.M. and Boski T. (2012).Enrichment of rare earth elements as environmental tracers of contamination by acid mine drainage in salt marshes: A new perspective. *Marine Pollution Bulletin*, 64: 1799-1808.
- Hudson, M.J., 1982. An introduction to some aspects of solvent extraction chemistry in hydrometallurgy. *Hydrometallurgy* 9, 149–168.Jin
- Kaur, H., Agrawal, Y.K., 2005. Functionalization of XAD-4 resin for the separation of lanthanides using chelation ion exchange liquid chromatography. *React. Funct.* Suzuki, T., Itoh, K., Ikeda, A., Aida, M., Ozawa, M., Fujii, M., 2006. +

Koen Binnemans, Peter Tom Jones, Bart Blanpain, Tom Van Gerven, Yongxiang Yang, Allan Walton, Matthias Buchert. 2013. Recycling of rare earths: a critical review. *Journal of cleaner production*. 1-22.

Kynicky J., Smith M.P. and Xu C. (2012) Diversity of Rare Earth Deposits: The Key Example of China. *Elements*, 8: 361–367

Kumar Manis Jha, Archana Kumari, Rekha Panda, Jyothi Rajesh Kumar, Kyoungkeun Yoo. 2016. Review on hydrometallurgical recovery of rare earth metals. *Hydrometallurgy*. p77.

Kumar, B.N., Radhika, S., Reddy, B.R., 2010. Solid–liquid extraction of heavy rare-earths from phosphoric acid solutions using Tulsion CH-96 and T-PAR resins. *Chem. Eng. J.* 160 (1), 138–144.

Li, D.Q., Wang, Z.H., Meng, S.L., 1994. Recommended separation processes for ion-adsorbed rare earth minerals. *Hydrometallurgy'94*. Chapman Hall, London, UK, pp. 627–634.

Li, J., Huang, X., Zhu, Z., Long, Z., Peng, X., Cui, D., 2007a. Extracting rare earth from D2EHPA-HEHEHP-H<sub>2</sub>SO<sub>4</sub> system. *Journal of The Chinese Rare Earth Society* 25 (1), 55–58.

Li, W., Wang, X., Meng, S., Li, D., Xiong, Y., 2007b. Extraction and separation of yttrium from the rare earths with sec-octylphenoxy acetic acid in chloride media. *Hydrometallurgy* 54, 164–169.

Li, W., Wang, X., Zhang, H., Meng, S., Li, D., 2007c. Solvent extraction of lanthanides and yttrium from nitrate medium with CYANEX 925 in heptane. *Journal of Chemical Technology and Biotechnology* 82, 376–381.

Lu, J., Wei, Z., Li, D., Ma, G., Jiang, Z., 1998. Recovery of Ce (IV) and Th (IV) from rare earths (III) with Cyanex 923. *Hydrometallurgy* 50, 77–87.

Mason, G.W., Bilobron, I., Peppard, D.F., 1978. Extraction of U(VI), Th, (IV), Am (III) and Eu(III) by bis para-octyl phosphoric acid in benzene diluent. *Journal of Inorganic and Nuclear Chemistry* 40, 1807–1810.

Massari Stefania, Marcello Ruberti. 2013. Rare earth elements as critical raw materials: Focus on international markets and future strategies. *Resources Policy*. 36-43

Nag, K., Chaudhury, M., 1977. Thio- $\beta$ -diketonates of lanthanides—III synergistic solvent extraction behaviour of neodymium (III) with 1,1,1-trifluoro-4(2-thienyl)-4-mercaptobut-3-en-2-one (HSTTA) and some neutral donors. *J. Inorg. Nucl. Chem.* 39 (7), 1213–1215.

PANDA Nandita, Nihar Bala DEVI, Sujata MISHRA. 2014. Solvent extraction of praseodymium(III) from acidic nitrate medium using Cyanex 921 and Cyanex 923 as extractants in kerosene. *Turkish Journal of Chemistry*. 504-511.

PEPPARJD. D. F., P. FARISP., R. GRAYA ND G. W. MASON. 1958. STUDIES OF THE SOLVENT EXTRACTION BEHAVIOR OF THE TRANSITION ELEMENTS. I. ORDER AND DEGREE OF FRACTIONATION OF THE TRIVALENT RARE EARTHS. *Journal of Inorganic and Nuclear Chemistry* 7, 276–285.

Pinto, D.V.B.S., Martins, A.H., 2001. Electrochemical elution of a cation-exchange polymeric resin for yttrium and rare earth recovery using a statistical approach. *Hydrometallurgy* 60, 99–104.

Radhika, S., Nagaraju, V., Kumar, B.N., Kantam, M.L., Reddy, B.R., 2012. Solid–liquid extraction of Gd(III) and separation possibilities of rare earths from phosphoric acid solutions using Tulsion CH-93 and Tulsion CH-90 resins. *J. Rare Earths* 30 (12), 1270–1275.

Rice, A.C., Stone, C.A., 1962. Amines in Liquid–Liquid Extraction of Rare Earth Elements. US Bureau of Mines, R.I., p. 5923.

Sami Virolainen. 2013. HYDROMETALLURGICAL RECOVERY OF VALUABLE METALS FROM SECONDARY RAW MATERIALS. Lappeenranta University of Technology.

Stefania Massari , Marcello Ruberti. 2013. Rare earth elements as critical raw materials: Focus on international markets and future strategies. *Resources Policy*. 36-43.

Tatsuya Suzukia, Keisuke Itohb, Atsushi Ikedaa, Masao Aidaa, Masaki Ozawaa, Yasuhiko Fujii. 2004. Separation of rare earth elements by tertiary pyridine type resin. *J. Alloys Compd.* 408–412, 013–1016. *Polym.* 65, 277–283.

Tertre E., Castet S., Berger G. and Loubet M. and Giffaut E. (2005) Experimental sorption of Ni<sup>2+</sup>, Cs<sup>+</sup> and Ln<sup>3+</sup> onto a montmorillonite up to 150 C. *Geochimica et Cosmochimica Acta*, 69: 4937-4948

Thomas G. Goonan. 2011. Rare Earth Elements—End Use and Recyclability. U.S. Geological Survey, Reston, Virginia.

Tse, P.K., 2011. China's rare earth industry, U.S. Department of the Interior/U.S. Geological Survey. Open-file report 2011-1042

Wang, Y.C., Yue, S.T., Li, D.Q., Jin, M.J., Li, C.Z., 2002. Solvent extraction of scandium (III), yttrium (III), lanthanides (III) and divalent metal ion with secnonylphenoxy acetic acid. *Solvent Extraction and Ion Exchange* 20 (6), 701–706.

Xie Feng, Ting An Zhang, David Dreisinger, Fiona Doyle. 2014. A critical review on solvent extraction of rare earths from aqueous solutions. *Minerals Engineering*. 10-28.

Xiong, C., Meng, Y., Yao, C., Shen, C., 2009. Adsorption of Erbium(III) on D113-III resin from aqueous solutions: batch and column studies. *J. Rare Earths* 27 (6), 923–931.

Xiong, C., Zhu, J., Shen, C., Chen, Q., 2012. Adsorption and desorption of praseodymium (III) from aqueous solution using D72 resin. *Chin. J. Chem. Eng.* 20 (5), 823–830.

Xiong, C., Liu, X., Yao, C., 2008. Effect of pH on sorption for RE(III) and sorption behaviors of Sm(III) by D152 resin. *J. Rare Earths* 26 (6), 851–856.

Yang, X., Aijun Lin, Xiao-Liang Li, Yiding Wu, Wenbin Zhou, Zhanheng Chen. 2013. China's ion-adsorption rare earth resources, mining consequences and preservation. *Environmental development*. 131-136.

Yao, C., 2010. Adsorption and desorption properties of D151 resin for Ce(III). J. Rare Earths 28 (1), 183–188.

Zhu, L., Chen, J., 2011. Adsorption of Ce(IV) in nitric acid medium by imidazolium anion exchange resin. J. Rare Earths 29 (10), 969–973. Commercial Applications for Rare Earth Technologies, Rare Earth Industry and Technology Association 2009, <<http://www.reitusa.org/>>.

REE - Rare Earth Elements and their Uses, Geoscience News and Information, <http://geology.com/articles/rare-earth-elements/>.

## Annex

### A1. Experimental methodology

The concentration of arsenazo (III) solution must have  $2 \cdot 10^{-3}$  mold/dm<sup>3</sup>, and this archived by dissolving the solid compound into water. A buffer solution was created by dissolving 0, 1 mol of CH<sub>3</sub>COOH and 0,1 mol of NH<sub>4</sub>Cl in 1l of water and then add NaOH until a  $-\log[H^+]$  of 3.3 is archived. The samples used for the absorption detection with spectrophotometer was prepared by adding 19.5 ml of tampon solution, 0,5 ml of arsenazo(III) solution and 1 ml of samples with La(III) or Ce (III). A spectrophotometer UV-VISIBLE SPECTROPOTOMETER model UV-1603 from SHIMADZU was used



Figure x1 Samples of La (III) forming complex with arsenazo (III) in tampon solution

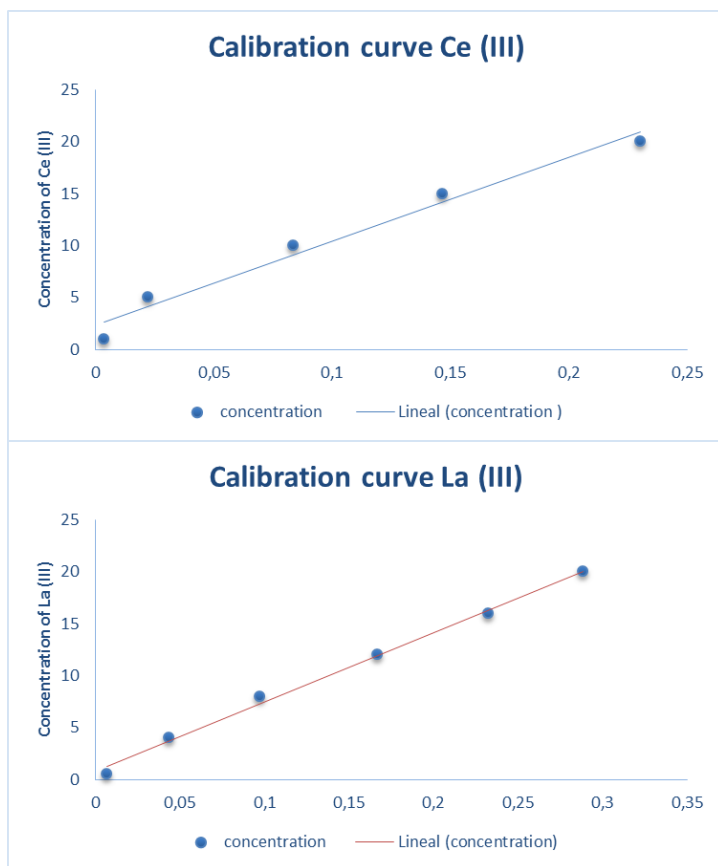


Figura x1 The calibration curve of Ce (III) and La (III)